



Spatial distributions, environmental drivers and co-existence patterns of key cold-water corals in the deep sea of the Azores (NE Atlantic)

Gerald Hechter Taranto^{a,b,*}, José-Manuel González-Irusta^{a,b,c}, Carlos Dominguez-Carrió^{a,b}, Christopher K. Pham^{a,b}, Fernando Tempera^{a,d}, Manuela Ramos^{a,b}, Guilherme Gonçalves^{a,b}, Marina Carreiro-Silva^{a,b}, Telmo Morato^{a,b}

^a Instituto de Investigação em Ciências do Mar – Okeanos, Universidade dos Açores, Horta, Portugal

^b IMAR Instituto do Mar, Universidade dos Açores, Horta, Portugal

^c Instituto Español de Oceanografía, Centro Oceanográfico de Santander, 39080, Santander, Spain

^d IFREMER, RBE/STH/LBH, Centre de Bretagne, Plouzané, France

ARTICLE INFO

Keywords:

Azores
Cold-water corals
Deep sea
Foundation species
Vulnerable marine ecosystems
Water masses

ABSTRACT

Habitat-forming cold-water corals (CWCs) represent a key component of deep-sea benthic communities and a priority target for conservation. Although research efforts have been mounting to try and identify the drivers of CWC distributions, progress has been limited by the scarcity of ecological data. The present work employs habitat suitability models (HSMs) to estimate spatial distributions, environmental drivers and co-existence patterns of 14 habitat-forming CWCs in the Azores, an area considered a hotspot of coral diversity in the Atlantic. The modelled CWCs showed a strong bathymetric zonation, which seems to be determined by the vertical stratification of water masses in the region. In particular, the modelled CWCs can be clustered in four groups named after the isopycnal (vertical) layers in which Atlantic water masses are organized: species restricted to upper water masses, species extending down from upper water masses, species restricted to intermediate water masses and species extending up from deep water masses. Horizontal patterns further indicate that the Azores Current and different production regimes north and south of the archipelago likely influence the distribution of CWCs in sub-surface waters. Such results have important implications for the regional management of deep-sea benthic communities and, in particular, for the design of representative networks of protected areas. The combined habitat of all modelled species covered only 11%. Given that they all possess the characteristics of benthic foundation organisms and represent indicator taxa of vulnerable marine ecosystems all the modelled species should be viewed as important targets for conservation. The lace coral *Errina dabneyi* deserves particular attention since this species appears to be endemic to the Azores and has a very limited estimated distribution.

1. Introduction

Data about the distribution of species, especially vulnerable and foundation species, are important to inform spatial management strategies and to better understand ecological and evolutionary processes (Hortal et al., 2015). However, distributional data in the deep sea tend to be scarce and species-environment relationships are often the proxy most commonly available to infer how species distribute in space and time. Thus, habitat suitability models (HSMs) that correlate available occurrence data and environmental parameters (Elith and Leathwick, 2009) are widely used tools to predict the geographic distribution of

deep-sea fauna.

The control of species distribution by abiotic conditions is one of the processes shaping biological communities (D'Amen et al., 2017; Vellend, 2010). In fact, abiotic conditions influence individual organisms and, together with biotic, stochastic, historical and evolutionary drivers, determine what groups of species are present or absent from specific areas (D'Amen et al., 2017; Kraft et al., 2015; Vellend, 2010). In general, the way abiotic conditions affect species distributions can be considered an intermediate process between those defining the regional pool of species and those structuring realized communities (Cornell and Harrison, 2014; D'Amen et al., 2017; Kraft et al., 2015). Only species able to

* Corresponding author. Instituto de Investigação em Ciências do Mar – Okeanos, Universidade dos Açores, Rua Prof. Dr. Frderico Machado, n.º 4, 9901-138, Horta, Portugal.

E-mail address: gh.taranto@gmail.com (G.H. Taranto).

<https://doi.org/10.1016/j.dsr.2023.104028>

Received 20 December 2022; Received in revised form 15 March 2023; Accepted 24 March 2023

Available online 27 March 2023

0967-0637/© 2023 The Authors. Published by Elsevier Ltd. This is an open access article under the CC BY-NC-ND license (<http://creativecommons.org/licenses/by-nc-nd/4.0/>).

tolerate similar environmental conditions can coexist in a particular area. Although it is challenging to distinguish the role of the environment from other drivers of spatial distributions (Cadotte and Tucker, 2017), a direct or an indirect role of the environment in the structuring of regional biodiversity can be expected if the environmental conditions of a region show a clear structure to which distinct pools of species can be linked to.

The distribution of habitat-forming cold-water corals (CWCs) is of particular interest for marine spatial managers and benthic ecologists for a number of reasons. Due to their specific life-history traits and consequent sensitivity to human-induced disturbance (e.g. Carreiro-Silva et al., 2013; Ragnarsson et al., 2017), habitat-forming CWCs have been defined as priority targets for conservation in several management initiatives. In Europe these include the EU Habitats Directive (92/43/EEC), the list of threatened and/or declining species and habitats of the OSPAR convention (Agreement, 2008–6) and the concept of Vulnerable Marine Ecosystems (VMEs) endorsed by the United Nations General Assembly (UNGA) together with the Food and Agriculture Organization (FAO, 2009). There is mounting evidence that CWC aggregations can influence localized current regimes (Cyr et al., 2016; Juva et al., 2020; Mienis et al., 2019; Soetaert et al., 2016), regulate nutrient flows (Cathalot et al., 2015; Georgian et al., 2016; Middelburg et al., 2016; Rix et al., 2016), and provide habitat to other benthic and demersal species (Buhl-Mortensen et al., 2010, 2017; Klompmaker et al., 2016; Linley et al., 2017). D'Onghia (2019) provides an interesting review on the role of CWCs as Essential Fish Habitat (EFH) given their important role as shelter, feeding and life-history critical habitats for fish species in the world oceans. Such key roles in ecological facilitation, community development and promotion of local biodiversity suggest that habitat-forming CWCs can be considered foundation species central to the development of deep-sea benthic communities (Crotty et al., 2019; Ellison, 2019; Orejas and Jiménez, 2017). Finally, CWCs likely contribute to regulating, supporting and provisioning ecosystem services (Thurber et al., 2014).

CWCs belong to a diverse polyphyletic group of sessile cnidarians that generally inhabit deep, aphotic and cold marine waters with most habitat-forming species belonging to the orders Scleractinia (stony corals) and Antipatharia (black corals), the subclass Octocorallia (soft corals, gorgonians and sea pens) and the family Stylasteridae (lace corals) (Roberts et al., 2009). They are all azooxanthellate (i.e., lacking symbiotic dinoflagellates), heterotrophs and characterized by the production of a calcium carbonate or proteinaceous supporting axis (Cairns, 2007; Roberts et al., 2009). CWCs are distributed globally down to depths of several thousands of meters with some species building large and long-lasting colonies that form extensive reefs or feature in dense 'deep-sea gardens' (Roberts et al., 2009). Their fascinating variety of shapes and colours and their sensitivity to human disturbances have contributed to put the deep sea in the spotlight of society's attention, research funds and conservation actions (Armstrong et al., 2019).

To date, 5.6% of the 3300+ CWC species estimated to exist worldwide (Roberts and Cairns, 2014) have been reported in the Azores region of the Mid-Atlantic Ridge (MAR), which comprises a mere 0.25% of the world's ocean (Braga-Henriques et al., 2013; Sampaio et al., 2019a). Such high species diversity establishes this region as an important biodiversity hotspot for CWCs with the subclass Octocorallia reaching the highest species diversity recorded so far in the North Atlantic (Sampaio et al., 2019a). Video surveys performed over the last decade using various underwater platforms (Morato et al., 2019b, 2020a, 2020b, e.g. 2021a; Orejas et al., 2017; Somoza et al., 2020) have reported dense aggregations of gorgonian, black and lace corals both on island slopes and offshore relieves. Reef-forming stony corals have also been reported in the Azores (i.e. *Desmophyllum pertusum*, *Madrepora oculata* and *Solenosmilia variabilis*) (Braga-Henriques et al., 2013; Sampaio et al., 2012), although the video footage available shows that down to 2000 m these species mostly exist as sparse colonies often embedded within multi-species coral gardens. Finally, there is only one

habitat-forming coral species that appears to be endemic to the Azores, the lace coral *Errina dabneyi* (Braga-Henriques et al., 2011; Zibrowius and Cairns, 1992).

Recognizing the ecological importance of habitat-forming CWCs and their prominence in hard-substrate communities throughout the region of the Azores, it is essential to investigate how these species distribute and what are the main environmental drivers shaping their distributions. The present work employs HSMS to estimate distributions, environmental drivers and co-existence patterns of some of the most common and vulnerable habitat-forming CWCs of the Azores, a hotspot of CWC diversity. Additionally, model predictions are used to assess if distinct pools of CWC taxa can be identified in the study region and if the spatial segregation of such pools can be associated to prominent environmental structures. The outputs of the present work will support and improve spatial management strategies in the region and will provide some insights into the ecology of these important species. All model outputs have been made available for download on the data repository PANGAEA (Taranto et al., 2023).

2. Methods

2.1. Study area

Comprising over one million km² on the northern MAR (Fig. 1a and b), the seascape of the Azores region is quite unique in the European context. Numerous volcanic islands, ridges and seamounts rise from an ocean floor reaching depths of several thousand meters and support different benthic habitats across a very broad bathymetric range (Mitchell et al., 2018; Peran et al., 2016; Tempera et al., 2012). Surface circulation is dominated by eastward currents originating from the Gulf Stream: (i) in the north there are branches of the North Atlantic Current, a current supporting the Atlantic Meridional Overturning Circulation; (ii) in the south there is the Azores Current that constitutes the northeast boundary of the North Atlantic subtropical gyre (Caldeira and Reis, 2017; Frazão et al., 2022; Sala et al., 2016). Both current systems are marked by intense vorticity with the Azores Current and its associated thermal front (the Azores Front) separating distinct production regimes (Frazão et al., 2022). The prevailing influence of the Azores high pressure system and the consequent sustained Ekman transport determine a confluence zone with different regimes northeast and southwest of the Archipelago (Caldeira and Reis, 2017), with potential implications for larval dispersal, marine colonization and speciation (Sala et al., 2016). Surface waters indicate a decreasing northwest-southeast gradient in productivity and other environmental parameters, with more productive waters located north and less productive waters located south of the archipelago (Amorim et al., 2017; Caldeira and Reis, 2017).

The different water masses present in the Atlantic Ocean have been recently described by Liu and Tanhua (2021) using conservative (temperature and salinity) and non-conservative (oxygen, silicate, phosphate and nitrate) water properties. Based on their work, at least eight water masses can be identified in the Azores (Fig. 2). Regional water masses present a complex stratification and can co-occur within specific depth intervals. Down to a depth of 2000 m, they can be divided into three isopycnal (vertical) layers: upper, intermediate and deep. Within the upper 400 m of the water column there are only upper water masses, whose relevance slowly decreases down to a depth of 1200 m (Fig. 2a–c). Intermediate water masses roughly occupy depths between 400 and 1600 m (Fig. 2d–e), with their strongest signature at about 800 m depth. Fractions of water masses characterizing the deep layer may occur as shallow as 400 m depth and extend to the deepest portion of the study area (2000 m) (Fig. 2g–i). Their strongest signature is located at about 1600 m depth. These patterns tend to be in accordance with the vertical stratification of water masses described for the Azores region in previous studies, although two main differences can be highlighted: (i) previous studies reported in the northwestern portion of the study area the Subarctic Intermediate Water (SAIW), however, given the lack of

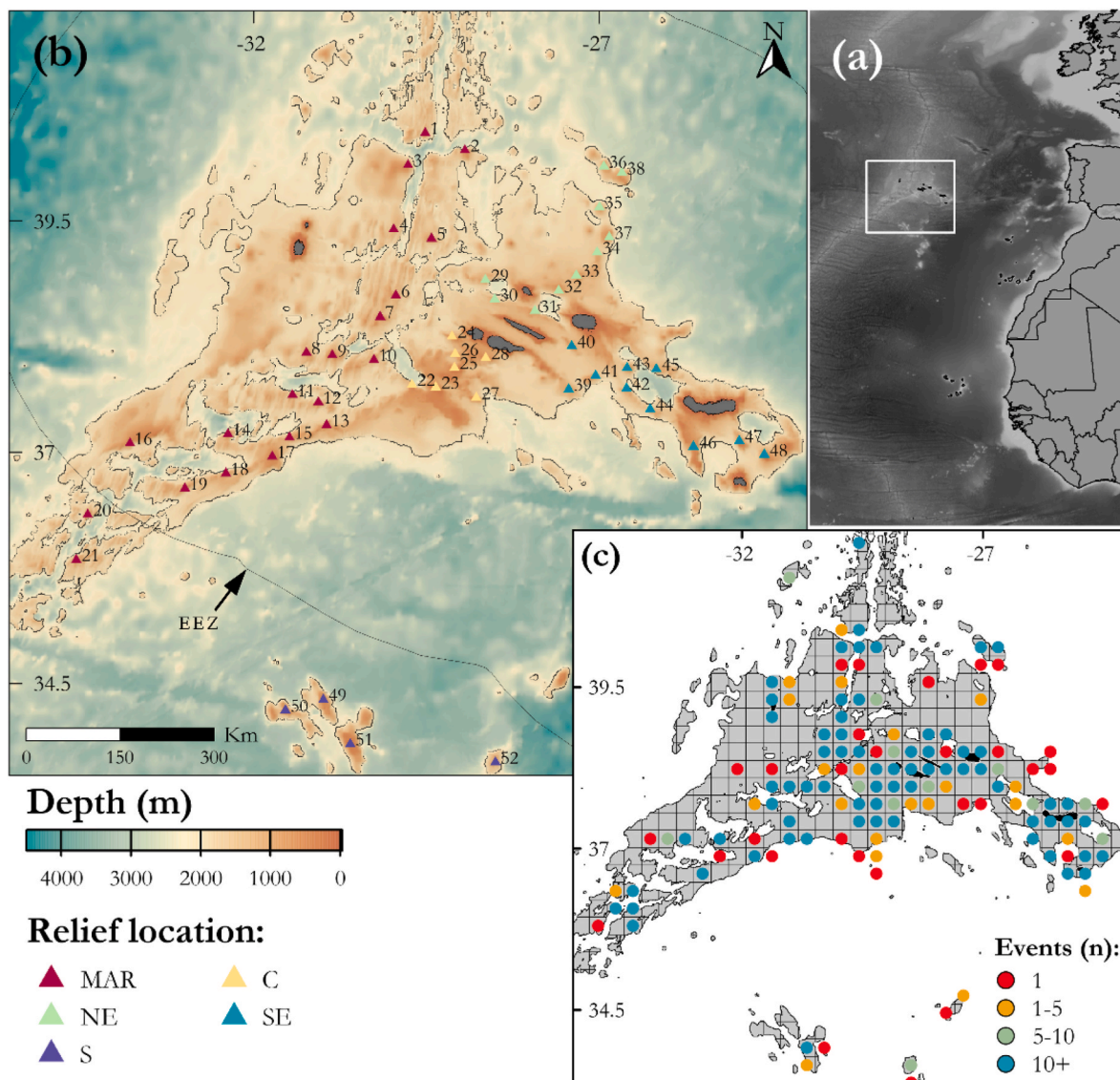


Fig. 1. Map of the study area. (a) Position of the Azores in NE Atlantic. (b) General bathymetry of the Azores. The islands (shown in dark grey) are from west to east: Flores, Corvo, Faial, Pico, São Jorge, Graciosa, Terceira, São Miguel and Santa Maria. The contour lines identify the spatial extent of the habitat suitability models, which consider only seafloor locations shallower than 2000 m. (c) Number of sampling events within the modelled area aggregated on a 30x30 km grid. Sampling events include video transects, longline surveys and bycatch data from fishing observers. Important regional underwater features: (1) Kurchatov N, (2) Kurchatov SE, (3) Kurchatov SW, (4) Agulha Corvo Graciosa, (5) Oscar, (6) Gigante, (7) 127sm, (8) Beta, (9) Cavala, (10) Ferradura, (11) Picoto, (12) Alfa, (13) Voador, (14) A3, (15) Monte Baixo, (16) Faial, (17) Monte Alto, (18) Farpas, (19) Cavalo, (20) Rainbow S, (21) Rainbow N, (22) Princess Alice W, (23) Princess Alice, (24) Condor, (25) Açor, (26) Condor de Fora, (27) De Guerne, (28) Baixo de São Mateus, (29) Graciosa West, (30) Perestrelo Bartolomeu, (31) Ilha Azul, (32) Mar da Fortuna, (33) Serreta, (34) João Leonardes, (35) Gaillard, (36) Sedlo, (37) Borda, (38) L'Espérance, (39) Albatroz do Meio, (40) São Jorge de Fora, (41) Albatroz do Norte, (42) Ferrara Northwest, (43) Dom João de Castro, (44) Ferrara, (45) Alcatraz, (46) Mar da Prata, (47) Grande Norte, (48) Formigas, (49) Atlantis N, (50) Atlantis NW, (51) Atlantis, (52) Tryo. The location of each underwater features is color coded: Mid-Atlantic Ridge (MAR), Central Seamounts (C), Northeastern Seamounts (NE), Southeastern Seamounts (SE) and Southern Seamounts (S). EEZ: Exclusive Economic Zone.

sampling stations in this area (Fig. 2f) it was almost absent in the data provided by Liu and Tanhua (2021); (ii) based on Liu and Tanhua (2021), the Mediterranean Water (MW) extends into the western portion of the study area (Fig. 2d), while previous works had suggested that this water mass was mostly limited to the eastern portion of the Azores region (Bashmachnikov et al., 2015; Johnson and Stevens, 2000).

2.2. Spatial resolution and modelling software

Models were built using a model grid having a cell size of a 1.13 x 1.11 km (i.e. about 0.01° in the UTM zone 26N projection). This resolution was considered a good compromise between the original resolution of occurrence and environmental data and our capacity to resolve

suitable and unsuitable areas within the same geomorphological feature using model predictions. Grid harmonization required the downscale of depth-derived variables and the upscale of environmental variables using bilinear interpolation (see Section 2.5). In order to mitigate sampling bias and model extrapolations (Phillips et al., 2009), study area and model background were limited to depths shallower than 2000 m where most of the sampling events took place (Fig. 1c). All analyses were performed in the R environment (version 4.2.0) (R Core Team, 2022).

2.3. Selection of CWCs and occurrence data

Fourteen CWC taxa (Fig. 3) representing some of the most common coral engineers found in regional hard-substrate communities were

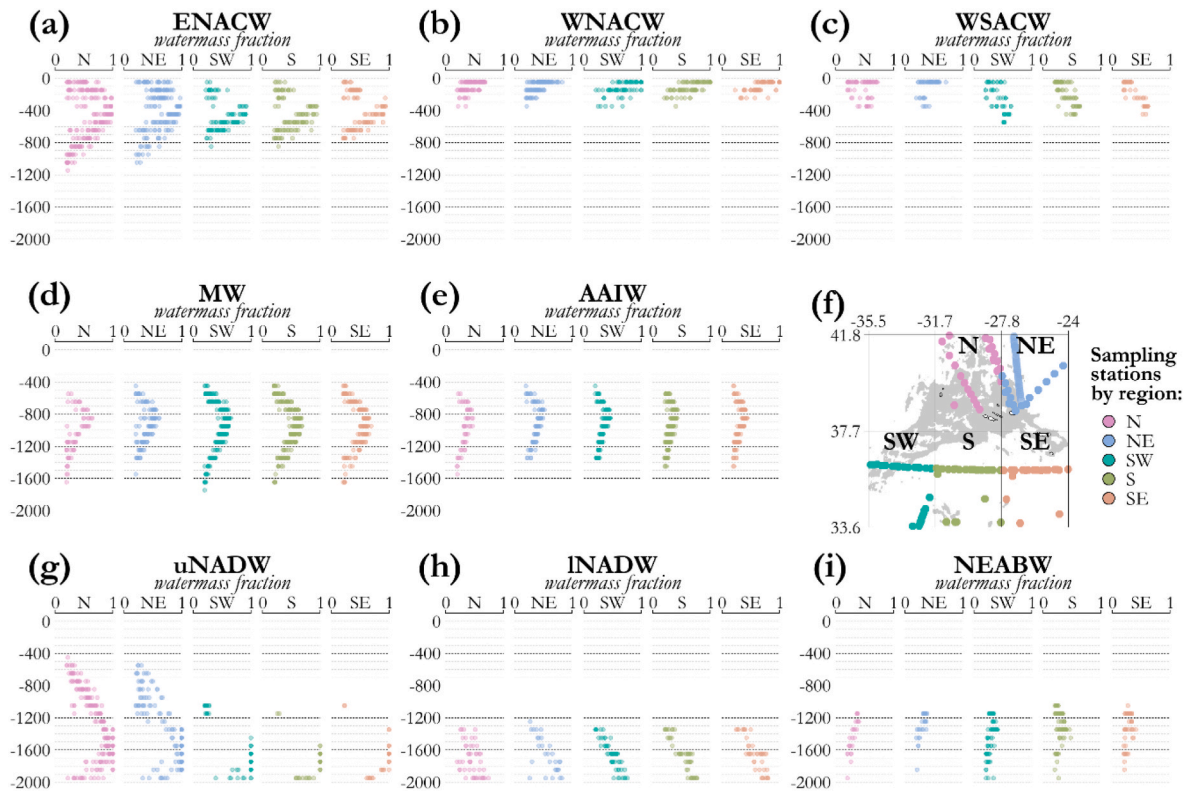


Fig. 2. Principal water masses of the Azores based on Liu and Tanhua (2021). Upper layer: (a) Eastern North Atlantic Central Water (ENACW), (b) Western North Atlantic Central Water (WNACW), (c) Western South Atlantic Central Water (WSACW). Intermediate layer: (d) Mediterranean Water (MW), (e) Antarctic Intermediate Water (AAIW). Deep and overflow layer: (g) Upper North Atlantic Deep Water (uNADW), (h) Lower North Atlantic Deep Water (INADW), (i) Northeast Atlantic Bottom Water (NEABW). Every sampling station is divided in 100 m bins over which water mass fractions are averaged. Only fractions greater than 0.2 are shown on the plots. (f) Sampling stations available in the study area; the grey background identifies seafloor depths shallower than 2000 m.

selected to build HSMs following the expert-driven approach described in Appendix A. Preliminary analyses of underwater video images showed that all selected species form monospecific or mixed coral gardens in the Azores (Morato et al., 2019b, e.g. 2021b). In addition, they are vulnerable to human activities (Carreiro-Silva et al., 2013; Morato et al., 2021b), appear to influence nutrient regimes (Rovelli et al., 2015, 2022), provide essential habitat to fish species (Gomes-Pereira et al., 2017) and one species (*Errina dabneyi*) may have a limited spatial distribution since it seems to be endemic to the region (Braga-Henriques et al., 2013; Zibrowius and Cairns, 1992). Models were built at genus or family level when identifications to species level were difficult (see Appendix A).

Presence records were obtained from two different sources: species annotations from underwater imagery and longline and handline bycatch records (Figures A1 and A.2). Most presence records (76%) came from annotations of video images collected through several scientific campaigns performed in the region by means of different platforms (Table 1), including ROVs, towed cameras and the Azor drift-cam (Dominguez-Carrió et al., 2021). By-catch records (24%) came from the Azores' Marine Biological Reference Collection database (COLETA), which compiles information from: (i) bycatch obtained from regional longline surveys on-board the N/I "Arquipélago" and (ii) bycatch collected under regional observer programs (Sampaio et al., 2019b). The positional accuracy of bycatch data was increased by: (i) retaining only presence records associated to georeferenced segments shorter than 1.5 km so that positional errors were comparable to the resolution of the model grid and (ii) discarding bycatch records with no reported depth or with a depth mismatch of more than 200 m with respect to our reference bathymetric grid (EMODnet, 2018).

2.4. Pseudo-absences and background points

Models were trained using a sampling bias corrected set of 10,000 pseudo-absences and background points (following Barbet-Massin et al., 2012; Phillips et al., 2009). As the sampling-bias was mostly depth related, raster locations were grouped into five depth strata and the probability of selection of pseudo-absences and background points was correlated to the sampling effort that occurred in each depth stratum as in Morato et al. (2020c). The geographic region for the generation of generalized additive model (GAM) pseudo-absences was further limited using environmental profiling based on presence data (function *OCSVMprofiling* from the R package MOPA; Iturbide et al., 2018) as in Morato et al. (2020c). The nu (or ν) parameter of *OCSVMprofiling* controls the error percentage of suitable locations misclassified as unsuitable by a support vector machine classifier – the higher the value of nu , the higher is the error tolerance (Drake et al., 2006; Schölkopf et al., 2001). The nu parameter was set to a value of 0.9 because with lower nu values pseudo-absences were not generated over large regions and this resulted in over-predicting models.

2.5. Environmental predictors

The candidate environmental predictors considered in this study are presented in Table B1. Following the approach adopted in similar studies (e.g. Davies and Guinotte, 2011; Georgian et al., 2019; Yesson et al., 2012) candidate predictors included: (i) depth and depth-derived layers, (ii) carbon export to the seafloor measured as particulate organic carbon (POC) flux and near-seafloor values of (iii) physical variables (iv) nutrient concentrations and (v) aragonite and calcite saturation levels. Bathymetric data were downloaded from EMODnet (EMODnet, 2018). Depth-derived layers were computed using the Benthic Terrain Modeler



Fig. 3. Habitat-forming cold-water corals selected to develop habitat suitability models in the Azores region. (a) *Callogorgia verticillata*, (b) *Narella bellissima*, (c) *Narella versluyisi*, (d) *Paracaliptrhophora josephinae*, (e) *Viminella flagellum*, (f) *Acanthogorgia* spp., (g) *Dentomuricea* aff. *meteor*, (h) Coralliidae, (i) *Paragorgia johnsoni*, (j) *Desmophyllum pertusum*, (k) *Madrepora oculata*, (l) *Solenosmilia variabilis*, (m) *Errina dabneyi*, (n) *Leiopathes* cf. *expansa*. © IMAR/Okeanos-UAz, Azor drift-cam (a, b, d, e, g, h, i, m); © iMAR cruise, iAtlantic & Eurofleets + projects, Okeanos-Uaz (c, j, n); © ROV Luso/EMEPC/2018 Oceano Azul Expedition, organized by Oceano Azul Foundation & partners (f); © ROV Luso/EMPEC (k, l).

toolbox in ArcGIS (Walbridge et al., 2018). Those variables included slope, bathymetric position index (BPI, a measure of the relative elevation of a location above the surrounding seafloor) calculated at two radii (5 and 20 km), ruggedness, eastness and northness (see Lecours et al., 2016; Lundblad et al., 2006). We computed POC flux based on Lutz et al. (2007) using the net primary productivity values reported in Amorim et al. (2017). Near-seafloor temperature, salinity and current speed were derived from the VIKING20 oceanographic model computed as the mean of monthly values for the period 1989–2009 (Böning et al., 2016). Near-seafloor nutrient concentrations were extracted from Amorim et al. (2017). Near-seafloor aragonite and calcite saturation levels were extracted from Wei et al. (2020).

Correlation and importance in preliminary models provided the criteria to identify the final set of environmental variables used in the HSMs. Correlation among predictors (Fig. 4) was maintained at acceptable levels ($r \leq 0.70$) (Dormann et al., 2013) by removing those variables less meaningful for coral distribution, as inferred from the literature. Depth was excluded because it represents an indirect predictor (Araújo et al., 2019) showing a high correlation with direct variables such as temperature. Nutrient concentrations and aragonite/calcite saturation levels were all highly correlated. Therefore, the number of such variables was reduced using the principal component analysis (PCA) (Dormann et al., 2013). This technique can be used on raster data to produce PCA maps, i.e. raster layers where to each pixel

Table 1

– Imaging surveys that provided the data used in the present study. ROV: remotely operated vehicle.

Cruise name	Vessel	Year	Platform	Reference
EMEPC/LUSO/G3	NRP Gago Coutinho	2008	ROV LUSO	https://www.emepc.pt/campanhas
Treasure 64PE388	RV Pelagia	2014	RV Pelagia tow-cam	–
Biometore	NRP Gago Coutinho	2015	ROV LUSO	Carreiro-Silva et al. (2015)
MEDWAVES	RV Sarmiento de Gamboa	2016	ROV Liropus	Orejas et al. (2017)
Treasure 64PE412	RV Pelagia	2016	RV Pelagia tow-cam	Duineveld (2017)
MapGES 2018	NI Arquipélago	2018	Azor drift-cam	Morato et al. (2019a)
Blue Azores 2018	NRP Gago Coutinho	2018	ROV LUSO	Morato et al. (2019b)
Nico 2018 Leg 12	RV Pelagia	2018	RV Pelagia tow-cam	Dominguez-Carrió et al. (2019b)
Greenpeace Pole-to-Pole	MV L'Esperanza	2019	ROV SEAEYE COUGAR-XT	Carreiro-Silva et al. (2019)
MapGES 2019	NI Arquipélago	2019	Azor drift-cam	Morato et al. (2020b)
Rainbow 64PE454	RV Pelagia	2019	RV Pelagia tow-cam	Dominguez-Carrió et al. (2019a)
iMAR 2021/ Eurofleets+	RV Pelagia	2021	RV Pelagia tow-cam	Morato et al. (2021a)

corresponds a value or score in a principal component dimension (Demšar et al., 2013; Dormann et al., 2013). PCAs performed independently for standardized nutrient concentrations and carbonate

saturation levels resulted in highly correlated first principal component maps ($r = 0.94$). Based on the fact that different water masses present different nutrient concentrations and saturation levels (e.g., Azetsu-Scott et al., 2010; Fontela et al., 2020; González-Dávila et al., 2011; Liu and Tanhua, 2021), these variables were joined into the same PCA. The resulting first principal component, explaining 90% of the variance, was used to produce a predictor layer meant to detect the eventual correlation existing between the distribution of CWCs and that of the regional water masses. Hereinafter this layer is referred to as 'seawater chemistry'. Figure B.1 shows the relationships of seawater chemistry with nutrient concentrations and aragonite/calcite saturation levels. Temperature and seawater chemistry ($r = 0.72$) were both maintained as predictor variables as they appeared to be relevant in preliminary model outputs. Finally, we excluded predictors that consistently showed little importance in preliminary models (sensu Thuiller et al., 2009) (i.e. eastness, northness and ruggedness).

The final set of predictors is plotted in Figure B.2 and includes: BPI (5 km and 20 km radii), slope, POC flux, seawater chemistry and near-seafloor values of current speed, oxygen saturation and temperature.

2.6. Habitat suitability models

Habitat suitability models (HSMs) were built using two approaches: generalized additive models (GAMs) (Hastie and Tibshirani, 1990) and maximum entropy models (Maxent) (Phillips et al., 2006). Models were built using the functions *gam* from the R package *mgcv* (Wood, 2011) and *maxent* from the R package *dismo* (Hijmans et al., 2022). GAMs were computed using a binomial family and a maximum basis dimension (k) equal to 4. Default parameters were used for Maxent models. Combined habitat suitability maps were produced based on the results of both

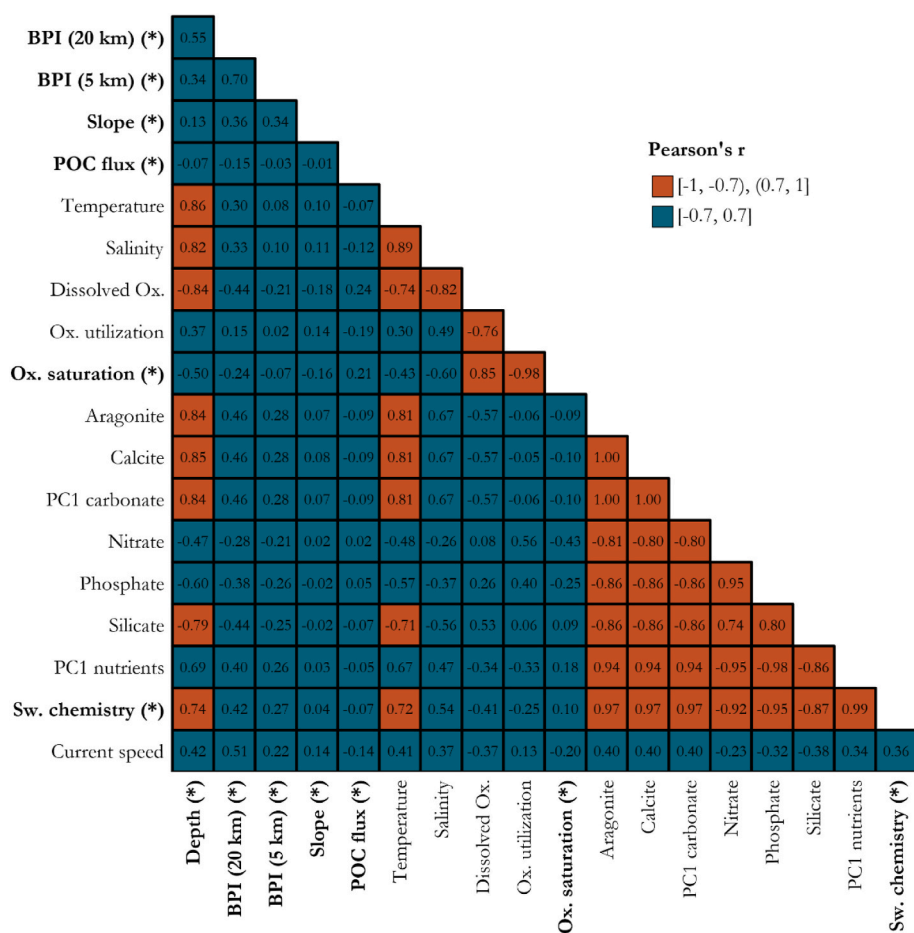


Fig. 4. Pearson's correlation coefficient (r) among all the considered predictor variables. The final set of predictor variables used in the modelling exercise is presented in bold and marked with (*). BPI: bathymetric position index; POC: particulate organic carbon; Ox.: oxygen, PC1 carbonate: first principal component of aragonite/carbonate saturation levels; PC1 nutrients: first principal component of nitrate, phosphate and silicate concentrations. Sw. chemistry: seawater chemistry, first principal component of nutrient concentrations and aragonite/carbonate saturation levels.

modelling approaches as described in the following paragraphs. Figure C.1 describes the general workflow followed to develop and evaluate HSMS and assess niche similarities.

From the final set of predictor variables, only a subset was used to build GAMs, while all predictor variables were used as Maxent model inputs. GAMs were fitted using all possible combinations of the predictor variables and the models presenting the lowest Akaike Information Criterion (AIC, Symonds and Moussalli, 2011) were selected (function *dredge* in the R package MuMIn, Bartoń, 2022). Variable importance was estimated following the permutation approach ($n = 100$) implemented by the function *variables_importance* (R package Biomod2) described in Thuiller et al. (2022, 2009). Response curves were built considering changes in habitat suitability indices (HSI) when a focal predictor varied at 100 points across its range while keeping all other predictors at their mean value (Elith et al., 2005). Finally, those variables that had a permutation importance greater than 10% and that ranked within the top four most important variables in both GAM and Maxent models were defined as shared important variables.

Model evaluation and confidence in model outputs were evaluated considering local and overall measures of performance and similarity as described below and summarized in Figure C.1.

Spatial autocorrelation. Spatial autocorrelation in model residuals was investigated using the global Moran's I coefficients (Dormann et al., 2007) computed with the R package *ape* (Paradis and Schliep, 2019). All Moran's I coefficients were close to zero and non-significant (p -value > 0.05).

Bootstrapping. The best GAM and Maxent models were built using all presence records and produced binary predictions based on the sensitivity-specificity sum maximization (MSS) threshold (Liu et al., 2005). Then, a bootstrap process ($n = 100$) evaluated the local confidence of model predictions. Each bootstrap iteration sampled occurrence data with replacement, fitted HSMS models and produced binary suitability maps based on the MSS threshold. Depending on the number of times individual raster cells were predicted as suitable they were classified as: low [1–30%), medium [30–70%) or high [70–100%] confidence suitable cells.

Cross-validation. Spatial block cross-validation is considered the best practice when no independent datasets are available to validate model predictions (Araújo et al., 2019). Presence and pseudo-absences/background points were assigned to different spatial blocks using the function *spatialBlock* (R package blockCV, Valavi et al., 2019). The function *spatialAutoRange* was used to define the block size (Valavi et al., 2019). Each block was then assigned randomly to one of five folds. One at a time, individual folds were left out for cross-validation while the remaining four were used for model fitting. Because the random grouping of spatial blocks into folds can influence the cross validation, the entire process was repeated five times setting different random seeds (5-seed 5-fold spatial block cross-validation). Averaged values of area under the curve (AUC) and true skill statistics (TSS) provided estimates of the overall performance of model predictions (Allouche et al., 2006). Using these statistics, models could be classified as good ($AUC > 0.8$; $TSS > 0.6$), fair ($0.7 \leq AUC \leq 0.8$; $0.4 \leq TSS \leq 0.6$) or poor ($AUC < 0.7$; $TSS < 0.4$) (Landis and Koch, 1977).

Fuzzy matching. The level of similarity between the spatial distribution of GAM and Maxent binary predictions (low-, medium- and high-confidence suitable cells) at a local (i.e. cell) level was measured considering two membership functions (Hagen, 2003): category similarity, which assumed that some categories were more similar than others (Table C.1); distance decay, which defined the fuzzy similarity of two cells as (i) identical if they matched perfectly, (ii) linearly decreasing with distance if the matching category was found within a 2-cell radius (~2 km) or (iii) totally different when no matching category was found within a 2-cell radius. Hagen (2003) provides the details to combine membership functions and compute local fuzzy similarity scores ranging from 0 (totally different) to 1 (identical). Values of fuzzy similarity greater than 0.5 indicate raster cells that are more similar than

different.

Improved Fuzzy Kappa. The overall similarity between GAM and Maxent predictions was measured using two Improved Fuzzy Kappa scores (Hagen-Zanker, 2009): (i) the first measured the overall correspondence of high-, medium- and low-confidence suitable cells of GAM and Maxent predictions (F_k); (ii) the second measured only the overall correspondence of high-confidence suitable cells (F_{kHC}). Areas consistently predicted as suitable with high confidence by both modelling approaches were considered the best suited to characterize CWC habitats. Therefore, the overall level of similarity of model predictions was determined using the F_{kHC} index and classified as good ($F_{kHC} > 0.6$), fair ($0.4 \leq F_{kHC} \leq 0.6$) or poor ($F_{kHC} < 0.4$) following the classification adopted for Kappa type statistics (Landis and Koch, 1977).

Finally, CWC distributions were estimated based on suitability maps that combined GAM and Maxent predictions. Models could be classified as good, fair or poor based on performance (AUC and TSS) and similarity scores (F_{kHC}). Overall confidence (OC) scores of combined habitat suitability maps were determined by the score resulting in the worse model classification among AUC_{GAM} , TSS_{GAM} , AUC_{Maxent} , TSS_{Maxent} and F_{kHC} . Suitable raster cells of combined habitat suitability maps were classified as follows.

- i. *High-confidence suitable cell*: raster cell predicted as suitable with high confidence by both GAM and Maxent;
- ii. *Medium-confidence suitable cell*: raster cell predicted as suitable with medium or high confidence by GAM, Maxent or both and with a local fuzzy similarity greater than 0.5;
- iii. *Low-confidence suitable cell*: any other cell predicted as suitable by GAM and/or Maxent.

2.7. Niche equivalence and similarity

Pair-wise niche overlaps were measured using the Schoener's D which ranges from 0 (no overlap) to 1 (complete overlap) (Warren et al., 2008). Niches were quantified considering only the environmental conditions occurring at the high-confidence suitable cells of the combined habitat suitability maps. Only variables describing water properties were used to quantify the niche space (i.e. seawater chemistry, POC flux and near-seafloor values of temperature, oxygen and current speed). The goal was to verify whether distinct pools of CWCs could be identified based on seawater properties alone.

Niche analyses were implemented using the R package *humboldt* and the Schoener's D was computed in the environmental space to reduce possible geographic biases in habitat availability (Brown and Carnaval, 2019). The total environmental space was bounded by the environmental ranges found across the combined high-confidence suitable cells of all modelled CWC taxa. The environmental dimensions were reduced using the principal component analysis and the first two components were considered to quantify the niches occupied by different species. The principal components were projected on a grid of 100 x 100 cells and a kernel density function was used to determine the smoothed density of occurrences in each cell of the grid (Brown and Carnaval, 2019). The analysis corrected the occurrence densities of each species by the prevalence of the environments in their range (Brown and Carnaval, 2019) and removed duplicate suitable cells in buffers of 5 km (distance chosen based on the spatial autocorrelation ranges of the environmental layers, function *spatialAutoRange* from the R package block CV, Valavi et al., 2019). The corrected densities of occurrences were used to measure the niche overlap of different species. We used the equivalence statistic to assess whether the ecological niches of pairs of CWCs were significantly different from each other. The observed Schoener's D value was compared to values obtained when the occurrences of the two species were resampled (200 times). Significance was determined by the number of times the observed overlap was greater than the overlap of the reshuffled datasets. The hypothesis of niche equivalency was rejected with p -values < 0.05 . We used the background statistic to assess if the

niche overlap of two species was more similar than expected by chance given the underlying environmental conditions. The statistic compared the similarity of the niches of species 1 and 2 to the similarity of species 1 and the random shifting of the spatial distribution of species 2 (and vice versa). The process is repeated 200 times and if the simulated overlap is consistently lower than the observed overlap (p -value < 0.05) then the background test is significant. See Brown and Carnaval (2019) for more details.

3. Results

3.1. Model evaluation

Evaluation scores are shown in Table 2. Overall confidence scores, determined considering both performance and similarity of GAM and Maxent predictions, were good for 8 taxa (*Acanthogorgia* spp., *Callogorgia verticillata*, Coralliidae spp., *Dentomuricea* aff. *meteor*, *Narella bellissima*, *Narella versluysi*, *Paragorgia johnsoni* and *Viminella flagellum*) and fair for 6 (*Errina dabneyi*, *Desmophyllum pertusum*, *Leiopathes* cf. *expansa*, *Madrepora oculata*, *Paracalyptophora josephinae* and *Solenosmilia variabilis*). No model showed poor performance (AUC and TSS) nor poor similarity (F_{kHC}) scores. Similarity scores were good for 9 taxa (*Acanthogorgia* spp., *C. verticillata*, Coralliidae spp., *D. pertusum*, *D. aff. meteor*, *N. bellissima*, *N. versluysi*, *P. johnsoni* and *V. flagellum*) and fair for 5 (*E. dabneyi*, *L. cf. expansa*, *M. oculata*, *P. josephinae* and *S. variabilis*). On average, the overall similarity of model predictions increased when only high-confidence cells were considered (average $F_{kHC} = 0.63$; average $F_k = 0.5$). This suggests that similar areas were consistently predicted as suitable by both modelling approaches. The only exceptions were the taxa with the lowest sample size: *E. dabneyi* ($N = 23$; $F_{kHC} = 0.59$; $F_k = 0.58$), *S. variabilis* ($N = 24$; $F_{kHC} = 0.47$; $F_k = 0.46$) and *P. josephinae* ($N = 24$; $F_{kHC} = 0.54$; $F_k = 0.63$) (Table 2). Maxent and GAM models showed very similar AUC and TSS scores, with Maxent models performing only slightly better. Most AUC and TSS scores could be classified as good, with only four exceptions classified as fair: *D. pertusum*, *L. cf. expansa*, *M. oculata* and *S. variabilis*. After removing duplicate presence records falling within the same model grid cell, the number of records ranged from 23 (*E. dabneyi*) to 161 (*V. flagellum* and *Acanthogorgia* spp.) (Table 2). Apparently, the overall confidence of the HSMs increased with sample size, with most models with more than 50 observations falling in the good evaluation range. Standard errors of AUC and TSS scores and the similarity score F_{kHC} also seemed to be correlated with sample size: standard errors decrease and similarity increases with increasing sample sizes (Figure D.1).

Table 2

GAM and Maxent model evaluations using performance (AUC and TSS) and similarity (F_k and F_{kHC}) scores. Models can be classified as good (G), fair (F) or poor (P) based on each individual performance and similarity score. Overall confidence (OC) scores are determined by the score resulting in the worse model classification between AUC_{GAM} , TSS_{GAM} , AUC_{Maxent} , TSS_{Maxent} and F_{kHC} . Scores determining fair OC scores are highlighted in bold (no score determined poor OC scores). N: number of records; AUC: area under the curve; TSS: true skill statistics; F_k : improved fuzzy kappa; F_{kHC} : improved fuzzy kappa computed for high-confidence suitable cells. Note that F_k is presented only to allow for comparisons with F_{kHC} , but it is not considered to compute OC scores.

TAXA	N	TSS_{GAM}	AUC_{GAM}	TSS_{Maxent}	AUC_{Maxent}	F_k	F_{kHC}	OC
<i>Acanthogorgia</i> spp.	161	0.69 ± 0.12	0.90 ± 0.07	0.69 ± 0.12	0.90 ± 0.06	0.66	0.74	G
<i>C. verticillata</i>	98	0.68 ± 0.09	0.90 ± 0.04	0.69 ± 0.09	0.90 ± 0.04	0.42	0.75	G
Coralliidae	128	0.75 ± 0.10	0.92 ± 0.05	0.74 ± 0.10	0.91 ± 0.05	0.4	0.71	G
<i>D. aff. meteor</i>	51	0.76 ± 0.20	0.88 ± 0.14	0.80 ± 0.14	0.91 ± 0.09	0.38	0.64	G
<i>D. pertusum</i>	31	0.58 ± 0.21	0.78 ± 0.13	0.59 ± 0.17	0.79 ± 0.10	0.5	0.61	F
<i>E. dabneyi</i>	23	0.72 ± 0.23	0.85 ± 0.14	0.74 ± 0.19	0.85 ± 0.12	0.59	0.58	F
<i>L. cf. expansa</i>	46	0.60 ± 0.26	0.76 ± 0.24	0.62 ± 0.22	0.80 ± 0.17	0.32	0.58	F
<i>M. oculata</i>	63	0.61 ± 0.15	0.82 ± 0.10	0.59 ± 0.11	0.81 ± 0.09	0.42	0.56	F
<i>N. bellissima</i>	42	0.74 ± 0.17	0.89 ± 0.08	0.74 ± 0.16	0.90 ± 0.07	0.59	0.67	G
<i>N. versluysi</i>	58	0.73 ± 0.17	0.88 ± 0.08	0.74 ± 0.17	0.89 ± 0.08	0.53	0.62	G
<i>P. josephinae</i>	24	0.86 ± 0.14	0.93 ± 0.07	0.85 ± 0.13	0.93 ± 0.08	0.63	0.54	F
<i>P. johnsoni</i>	51	0.83 ± 0.09	0.94 ± 0.04	0.79 ± 0.08	0.93 ± 0.04	0.53	0.66	G
<i>S. variabilis</i>	24	0.66 ± 0.20	0.80 ± 0.13	0.69 ± 0.20	0.82 ± 0.11	0.47	0.46	F
<i>V. flagellum</i>	161	0.76 ± 0.07	0.93 ± 0.03	0.79 ± 0.06	0.94 ± 0.03	0.55	0.71	G
Average	69	0.71	0.87	0.72	0.88	0.5	0.63	–

Most of the raster cells predicted as suitable by GAM and Maxent models for octocorals were classified either as high- or medium-confidence suitable cells (Figures D.2 and D.3). The only octocoral taxa presenting a relevant percentage of low-confidence suitable cells were *C. verticillata* and *D. aff. meteor* in GAMs (Figure D.2a and g) and Coralliidae in Maxent (Figure D.3h), for which more than 50% of the cells were ranked as medium or low-confidence. These were also the taxa with the lowest local agreement between model predictions (Figure D.4a, g and h). The local agreement between the two modelling approaches seemed to be good for the remaining octocorals (Figure D.4).

Suitable habitats estimated by GAMs for Scleractinia, Antipatharia and Anthoathecata showed a proportion of high-, medium- and low-confidence cells similar to the results obtained for the octocoral taxa (Figure D.5). The only exception was *S. variabilis*, which presented a high percentage of medium-confidence cells (Figure D.5c). Maxent models appeared to be more influenced by the bootstrap process (Figure D.6) and to estimate larger suitable habitat for *L. cf. expansa*, *M. oculata* and *S. variabilis* when compared to the suitability maps produced by GAMs (Figures D.5 and D.6 b, c and e). Habitat suitability predictions had the lowest overlap for *L. cf. expansa* and *M. oculata*, while they improved for the remaining species (Figure D.7).

3.2. Variable importance and response curves

Variable importance for GAMs and Maxent models is shown in Fig. 5. The most important variable was seawater chemistry for both modelling approaches, with a median permutation importance of 29.6% for GAMs and 36.5% for Maxent models. It ranked among the most important variables for 12 out of the 14 modelled taxa. Among the depth-derived layers, the most relevant variables were BPI_20 km and slope. BPI_20 km ranked among the top four variables with a permutation importance greater than 10% five times for GAMs and eight times for Maxent models, and slope five times for GAMs and 12 for Maxent models. POC flux resulted important for most Maxent models, albeit it was relevant only for GAMs of three species: *Desmophyllum pertusum*, *Madrepora oculata* and *Leiopathes* cf. *expansa*. Near-seafloor water temperature was relevant for 9 of the modelled species: Coralliidae (GAM and Maxent), *D. pertusum* (GAM and Maxent), *Dentomuricea* aff. *meteor* (GAM and Maxent), *Errina dabneyi* (GAM and Maxent), *L. cf. expansa* (Maxent), *Narella bellissima* (GAM), *P. josephinae* (GAM), *Paragorgia johnsoni* (Maxent), *V. flagellum* (GAM and Maxent). The least important variables were BPI_5 km, current speed and oxygen saturation.

Response curves are shown in Figures D.8-15, presenting in most cases comparable results for both GAM and Maxent models. Responses

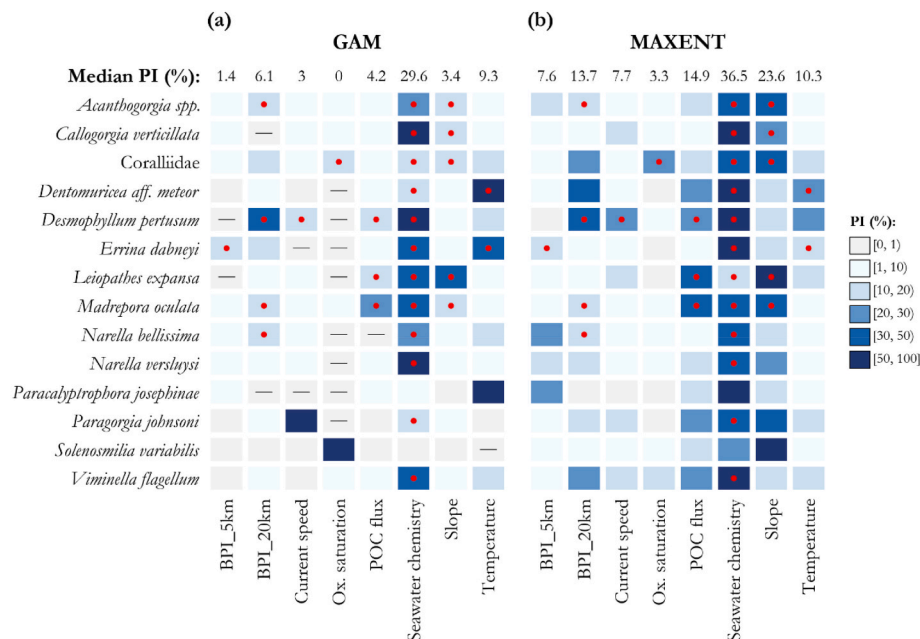


Fig. 5. Permutation importance (PI) of predictor variables for (a) GAM and (b) Maxent models. Dashes in (a) identify the variables *not* used to build GAMs; all variables were used for MAXENT models. Red dots identify shared important variables: variables that ranked within the top four and that had a permutation importance greater than 10% in both GAM and Maxent models. BPI: bathymetric position index; Ox. Saturation: oxygen saturation; POC flux: particulate organic carbon flux.

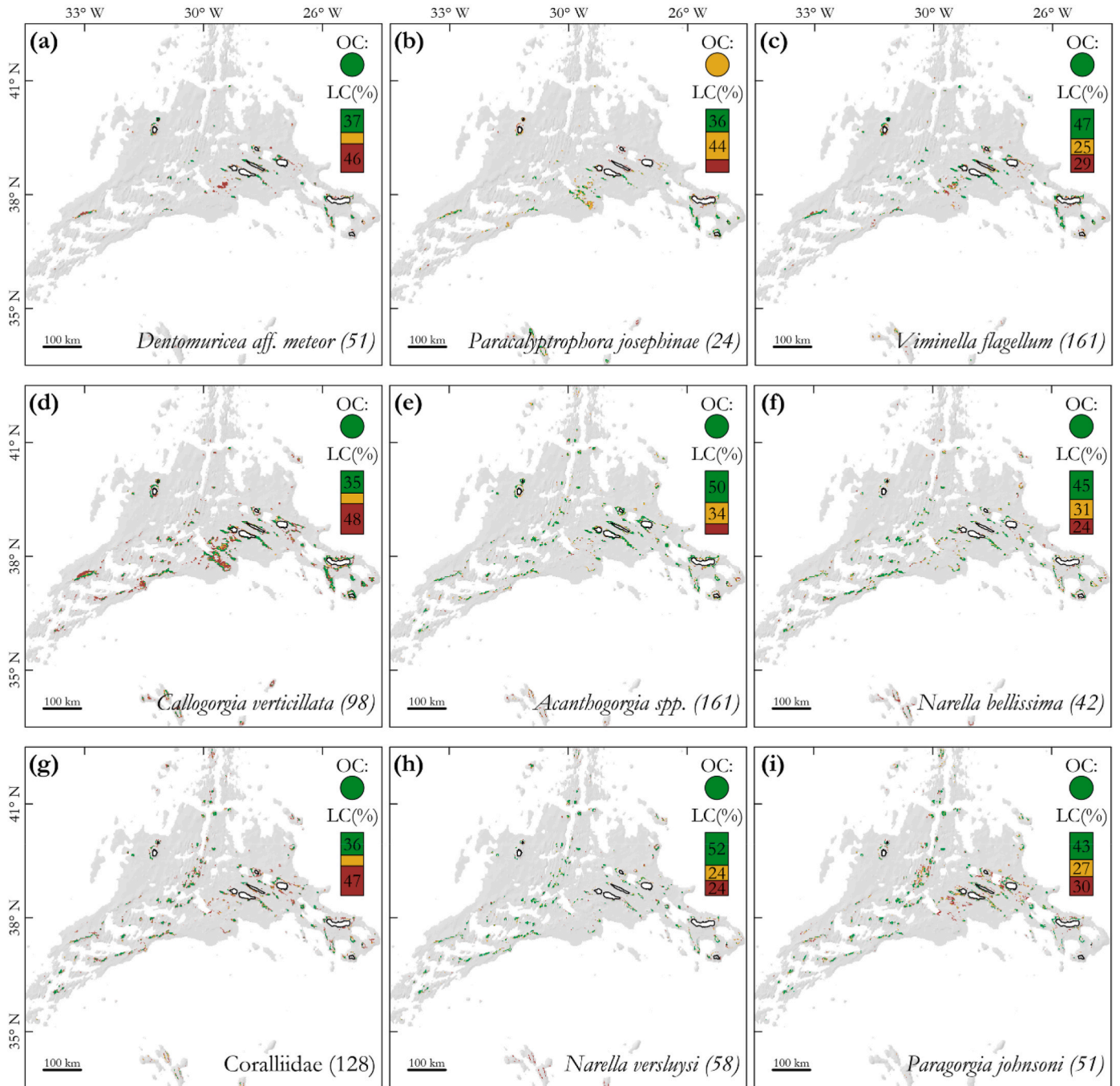
to the variable seawater chemistry could be roughly divided into two groups: ‘group 1’ associated to relatively high seawater chemistry values (*D. aff. meteor*, *E. dabneyi*, *P. josephinae*, *V. flagellum* and *Callogorgia verticillata* – Figure D.8 a-e); ‘group 2’ associated to relatively low seawater chemistry values (*N. bellissima*, *Narella versluysi*, *P. johnsoni*, *L. cf. expansa*, *D. pertusum*, *S. variabilis* and *M. oculata* – Figure D.8 g-n). *Acanthogorgia* spp. seemed to have responses in between these two groups. According to GAMs, three species of ‘group 1’ (*D. aff. meteor*, *E. dabneyi* and *P. josephinae*) displayed a narrow thermal range (Figure D.9 a-c), while Maxent responses showed, in general, wider tolerance ranges. *C. verticillata* appeared to have its optimal conditions slightly below 10 °C, showing wider tolerance ranges than other species of ‘group 1’ (Figure D.9 d). For *V. flagellum*, the optimal temperature appeared to be about 8 °C (Figure D.9 e). For octocorals and black corals of ‘group 2’, the optimal temperature was roughly between 5 and 10 °C, while the scleractinian species either had an unimportant (*S. variabilis* and *M. oculata*) or a positive relationship with temperature (*D. pertusum*) (Figure D.9 i-n). POC flux was a shared important variable for three species: *L. cf. expansa*, *D. pertusum* and *M. oculata* (all showing a positive relationship with POC flux) (Figure D.10 k-m). This variable had little importance for the remaining GAMs, while it was relevant for most Maxent models. Almost all taxa of ‘group 2’ (Figure D.10 i-n) as well as *D. aff. meteor*, *Acanthogorgia* spp. and Coralliidae spp. (Figure D.10 a, f and g) avoided areas of low carbon fluxes. *P. josephinae* and *V. flagellum* had a bell-shaped response curve centered on low and intermediate flux values, respectively (Figure D.10 c, e). POC flux was not relevant for the remaining models. The taxon Coralliidae was the only showing a significant response to oxygen saturation both in GAM and Maxent models, with suitability indices inversely correlated with saturation values (Figure D.11 g). Oxygen saturation was the only variable with high permutation importance for the GAM model of *S. variabilis* (Figure D.11 n). According to the Maxent model, the habitat available for *V. flagellum* decreased with increasing oxygen saturation values (Figure D.11 e). The habitat suitability index of almost all species was positively correlated with slope and fine scale bathymetric position index (BPI_5 km) values (Figures D.12 and D.13). Most species preferred high values of the coarse bathymetric position index (BPI_20 km) (Figure D.14) with the

exception of Coralliidae, *P. johnsoni*, and *M. oculata*, both associated to high and low BPI values (Figure D.14 g, j, m). Bottom current speed appeared to have some relevance only for *D. pertusum*, whose suitability index increased with increasing values of current speed (Figure D.15 l).

3.3. Spatial distributions and pools of CWC taxa

Considering high-confidence suitable cells of the combined habitat suitability maps (Figs. 6 and 7), the potential habitat of the modelled CWCs covered about 22,000 km², thus 11% of the modelled area. When considering also medium- and low-confidence suitable cells this percentage increased to 21 and 31%, respectively. High-confidence suitable cells of the combined habitat suitability maps identify the areas where we have the highest confidence in model predictions, therefore, unless differently stated, spatial distributions are presented considering high-confidence suitable cells only. Most suitable habitat was found at depths shallower than 1500 m (Fig. 8b) in association with major underwater geological features (island slopes, seamounts or ridges) (Figs. 6 and 7). All species had patches of suitable habitat on both sides of the Mid-Atlantic Ridge (MAR), even though habitat suitable for *E. dabneyi* seemed almost absent west of the MAR (Fig. 7a). The scleractinian corals *D. pertusum*, *M. oculata* and the black coral *L. cf. expansa* showed some latitudinal gradient, with high-confidence suitable cells mostly located in the northern portion of the study area (Fig. 8a). Raster cells suitable for 9 or more species were small, patchy and scattered between the MAR (on most of the features highlighted in Fig. 1b), the Central Seamounts (especially Condor, Baixo de São Mateus, Princess Alice W and De Guerne) and the South Eastern Seamounts (especially São Jorge de Fora, Dom João de Castro, Mar da Prata and Ferraria) (Fig. 9). The North-eastern and the Southern Seamounts appeared to have a low CWC species richness, with the exceptions of Graciosa West and Ilha Azul (Fig. 9). All the features mentioned are highlighted in Fig. 1b. On island slopes, multi-species aggregations seemed more likely to occur west of Corvo, southwest of Flores, west of Faial, Graciosa and Terceira, the westernmost and the easternmost tips of São Jorge, south and east of Pico and east and west of São Miguel. Santa Maria seemed to be the island less likely to aggregate the modelled CWCs (Fig. 9). Depth was not included

Combined habitat suitability maps:



Local confidence (LC):

- High-confidence suitable cell
- Medium-confidence suitable cell
- Low-confidence suitable cell

Overall confidence (OC):

- Good
- Fair
- Poor

Coordinate System: WGS 1984 UTM 26N
 Liner Unit: Meter (1,000)
 Scale Factor: 0.9996
 Datum: WGS 1984

Fig. 6. Combined habitat suitability maps for the selected octocoral (Alcyonacea) taxa. Local confidence (LC): percentage of cells classified as high, medium or low confidence. Overall confidence (OC) is determined by the lowest score among AUC_{GAM} , TSS_{GAM} , AUC_{Maxent} , TSS_{Maxent} and F_{kHC} . AUC: area under the curve; TSS: true skill statistics; F_{kHC} : improved fuzzy kappa for high-confidence suitable cells. In parenthesis, the number of records used to train the models. Species are ordered according to the mean depth of their estimated suitable habitat.

Combined habitat suitability maps:

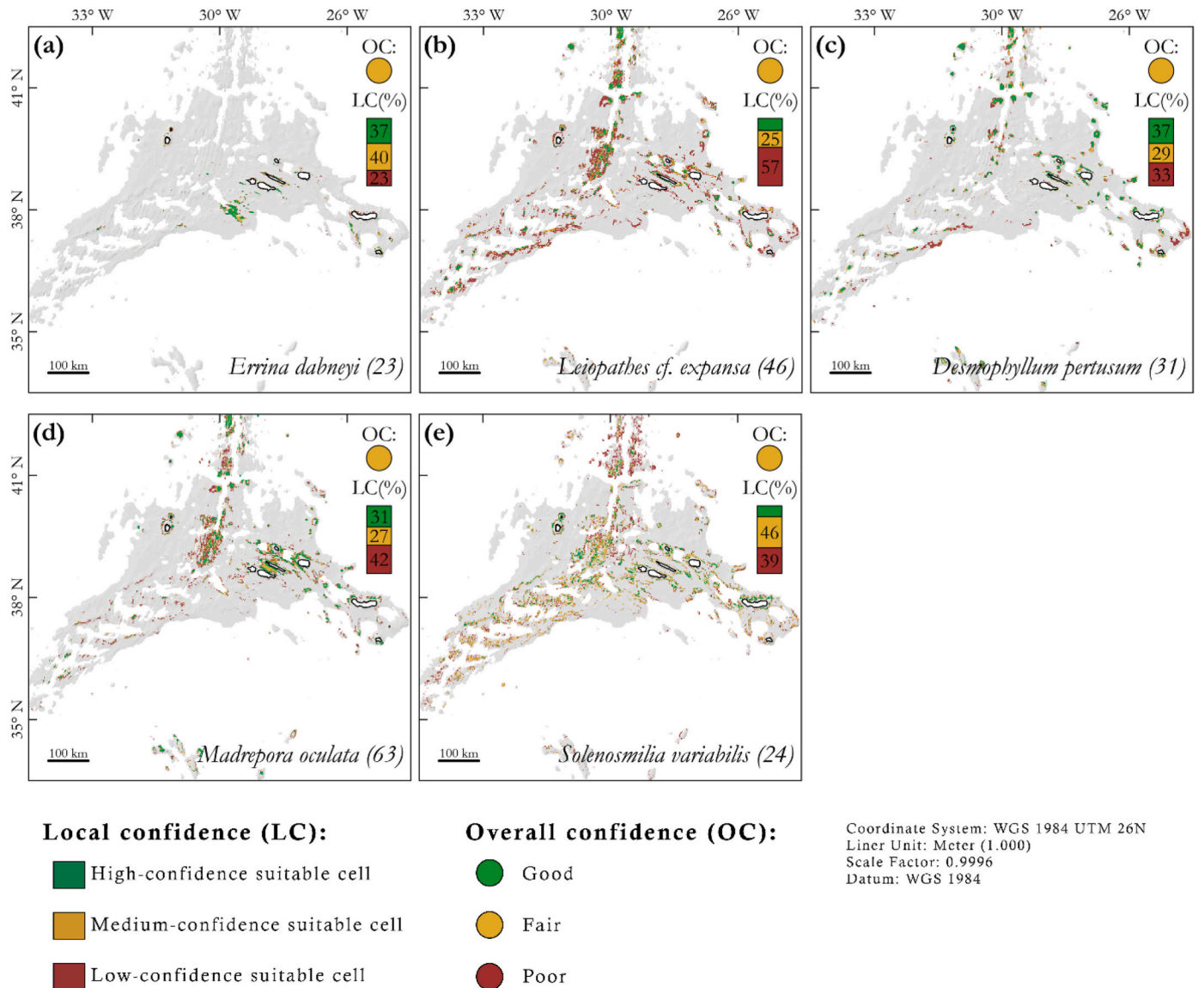


Fig. 7. Combined habitat suitability maps for the selected Anthothecata (Stylasteridae) (a), Antipatharia (b) and Scleractinia (c–e). Local confidence (LC): percentage of cells classified as high, medium or low confidence. Overall confidence (OC) is determined by the lowest score among AUC_{GAM} , TSS_{GAM} , AUC_{Maxent} , TSS_{Maxent} and Fk_{HC} . AUC: area under the curve; TSS: true skill statistics; Fk_{HC} : improved fuzzy kappa for high-confidence suitable cells. In parenthesis, the number of records used to train the models. Species are ordered according to the mean depth of their estimated suitable habitat.

as a predictor variable, yet habitat suitability model predictions showed a clear bathymetric zonation (Fig. 8b). Likely, this response was primarily mediated by the predictor seawater chemistry (Fig. 8c), the most important variable for both GAM and Maxent models (Fig. 5). Based on the response to seawater chemistry (Figure D.8), there appeared to be two distinct groups of CWCs (see Section 3.2). Complementing this information with the predicted horizontal and vertical distributions of CWCs, the modelled taxa could be divided into four groups whose distributions seemed correlated with the vertical stratification of regional water masses (see Fig. 2).

The first group of CWCs was mostly associated with areas shallower than 500 m depth, where water masses of the upper layer (UL) have their strongest signature. This group (UL-CWCs) included the species presenting the smallest estimated distributions: *E. dabneyi*, *P. josephinae* and *D. aff. meteor* (Fig. 6a–b, 7a and 8b), with *E. dabneyi* showing the smallest of all. Model predictions indicate that this species is mostly

limited to the central group of seamounts and islands and to the Southeastern Seamounts. Predictions for *P. josephinae* also covered a limited geographic area, yet it appeared to be more likely to occur in the southern portion of the MAR and in the Southeastern Seamounts when compared to *E. dabneyi*. It also covered part of the Southern Seamounts. The potential distribution of *D. aff. meteor* was similar to that of *P. josephinae*, however it had larger patches of suitable habitats associated with island slopes, especially around São Miguel, Terceira, Graciosa, São Jorge, Flores and Corvo. It appeared to be absent in the Southern Seamounts and in Santa Maria. These three species seemed virtually absent from the Northeastern Seamounts and from the northernmost portion of the MAR.

The second group of CWCs appeared to distribute mostly at seafloor locations bathed by water masses of the intermediate layer (IL), with high-confidence suitable cells presenting a median depth value corresponding to the core depth of the IL (ca. 800 m). This group (IL-CWCs)

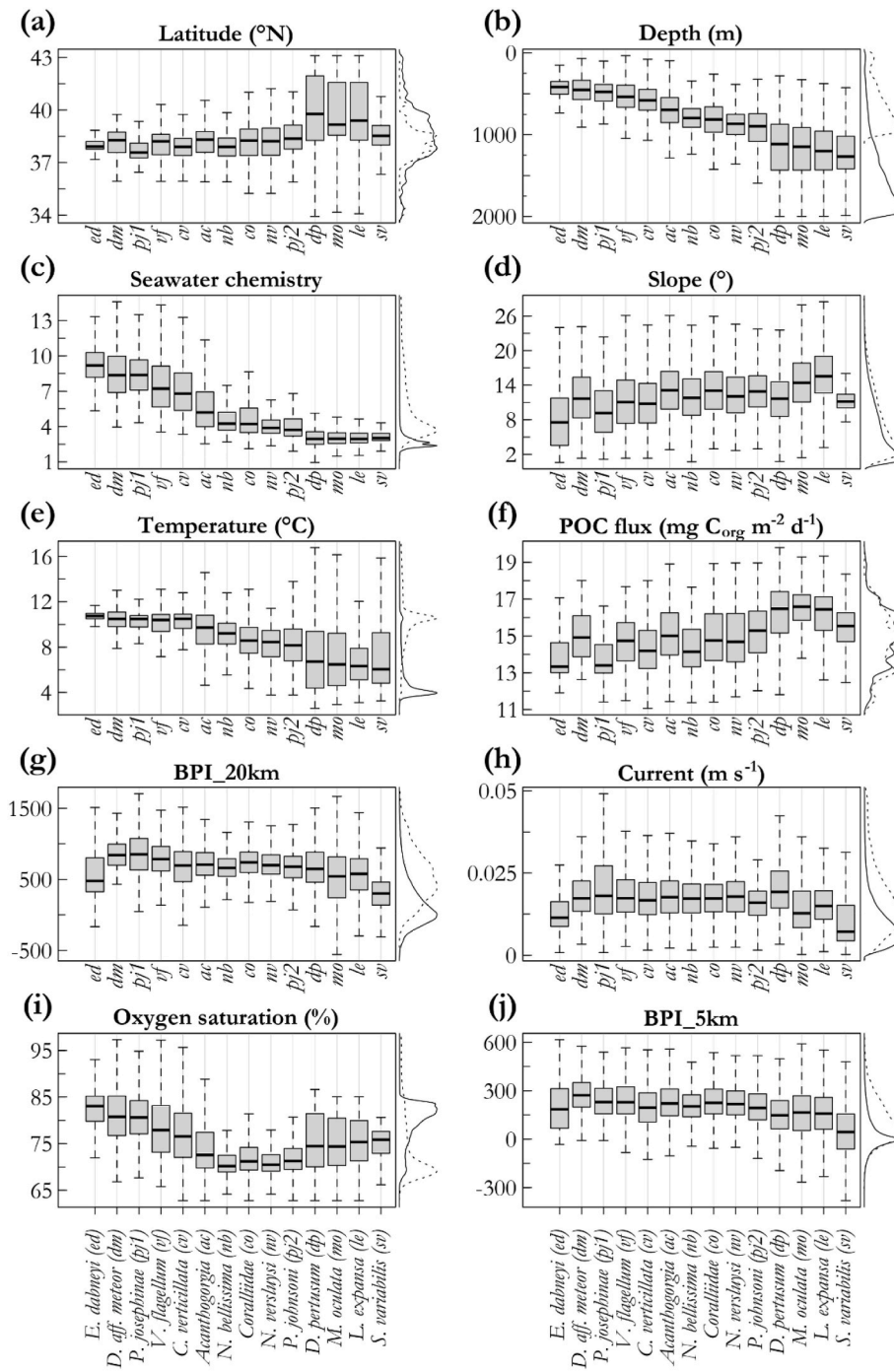


Fig. 8. Value ranges of relevant environmental variables determined by the high-confidence cells of the combined habitat suitability maps. (a) Latitude; (b) depth, in meters; (c–j) model predictors ordered by importance. Lines on the right side of the plots show the density distribution of each environmental predictor considering both suitable and unsuitable cells at seafloor in locations shallower than 2000 m (solid line) and shallower than 1000 m (dotted line). BPI: bathymetric position index; POC: particulate organic carbon. Note that latitude and depth were not used to develop HSMs.

included *N. bellissima*, *N. versluysi*, Coralliidae spp., and *P. johnsoni* (Fig. 6 f-i and 8b), which presented very similar geographic distributions and little overlap with UL-CWCs. The largest differences within IL-CWCs were: (i) the estimated habitat of *N. bellissima* covered a larger area in the Central Seamounts than the other taxa and it appeared to be almost absent north of Corvo Island, and (ii) *P. johnsoni* that presented the most limited estimated distribution and appeared to be absent from the Southern Seamounts. The most relevant zones of potential co-occurrence with UL-CWCs were: Gigante and the associated ridges, Cavala, Voador and Sarda on the MAR; Condor and De Guerne in the Central Seamounts; Mar da Prata and Grande Norte in the Southeastern Seamounts; island slopes west of São Miguel, Terceira and Corvo Islands and the tips of São Jorge Island.

The third group of CWCs (UIL-CWCs) included *V. flagellum*, *C. verticillata* and *Acanthogorgia* spp. (Fig. 6 c-e and 8b), which appeared to distribute mostly at seafloor locations shallower than 800 m depth, thus, at depths primarily influenced by upper and intermediate water masses. The combined suitable habitat of these taxa can be divided in two parts. The first part overlaps and includes almost entirely the combined suitable habitat of the UL-CWCs (with the exception of Princess Alice flat tops). The remaining portion of suitable habitat overlaps almost entirely with the combined suitable habitat of the IL-CWCs, even though the taxa of this group appeared able to inhabit areas unsuitable for UIL-CWCs. Considering each species individually, the habitat distribution of *V. flagellum* was very similar to the habitat distribution of UL-CWCs, although *V. flagellum* appeared to be virtually absent from

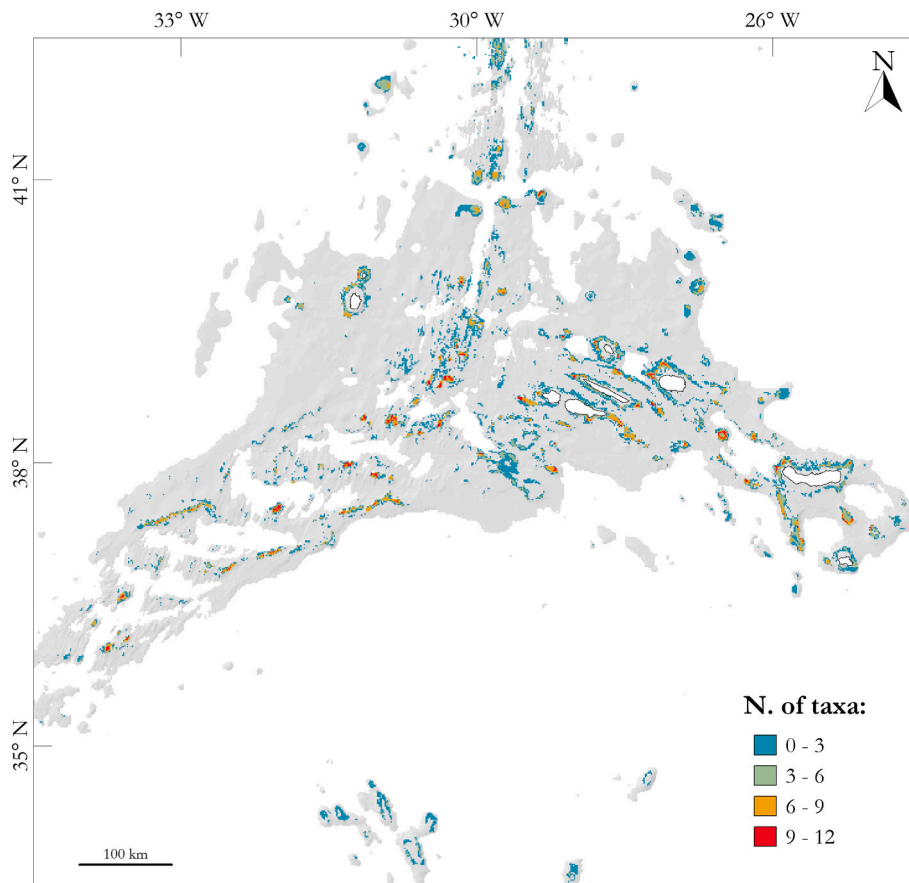


Fig. 9. Overlapping habitat suitability predictions for all modelled CWC taxa. Note that overlapping habitat suitability predictions are computed considering only high-confidence cells of combined habitat suitability maps.

Santa Maria. *C. verticillata* and *V. flagellum* presented similar predicted habitat distributions, yet *C. verticillata* seemed more likely to inhabit the Central and the Southern Seamounts than *V. flagellum* and presented suitable habitat predicted around Santa Maria. Based on model predictions, *Acanthogorgia* spp. seemed to prefer areas of steep slopes and to be able to inhabit larger portions of the MAR when compared to other UIL-CWCs (Figs. 6e–8d).

Finally, the fourth group of CWCs appeared to distribute mostly at seafloor locations deeper than 800 m depth, thus, at depths associated with the IL and with the deep layer (DL). This group (IDL-CWCs) included *D. pertusum*, *M. oculata* and *L. cf. expansa* (Fig. 7 b-d and 8b). The predicted suitable habitat of IDL-CWCs almost never overlapped with the combined suitable habitat of UL-CWCs and very rarely with UIL-CWCs. The most evident locations where this happened were: Gigante and associated ridges, Cavallo, Rainbow N and S on the MAR; Mar da Fortuna in the Northeastern Seamounts; Mar da Prata, Grande Norte, Dom João de Castro, Alcatraz in the Southeastern Seamounts; the island slopes of São Miguel, Terceira, Graciosa and Corvo. The habitat overlay was mostly due to *Acanthogorgia* spp. Overlapping habitats were more common among IL- and IDL-CWCs. The habitats of *D. pertusum*, *M. oculata* and *L. cf. expansa* were very scarce in the Central Seamount Group and on the slopes south of Pico and Faial while they appeared on most of the remaining geomorphic features highlighted in Fig. 1b.

Predictions and responses of *S. variabilis* (Fig. 7e), whose models were essentially fitted using bycatch data (Figure A.2c), seemed to be the least trustworthy, thus, were not associated with any particular group.

3.4. Pools of CWC taxa and regional environmental structures

Environmental values at locations of high-confidence suitable cells and background environmental values of the modelled region are shown in Fig. 10. Background values of near-seafloor concentrations of dissolved nutrients increase down to about 800 m depth and then they became almost constant down to about 2000 m depth. At 800 m depth, there exists the oxygen minimum zone of the study area. Temperature and saturation levels of aragonite and calcite decrease with depth, the decrease is gradual for the carbonate compounds and not homogeneous for temperature. The bathymetric zonation of the modelled CWCs seemed to be correlated with these environmental patterns. In particular, the IL-CWCs (*N. bellissima*, *N. verluysi*, Coralliidae spp., and *P. johnsoni*) were tightly associated to the regional oxygen minimum and to nutrient concentrations matching the transition from decreasing to constant background values (Figs. 8i and 10c). Note that the regional oxygen minimum levels do not go below 4.3 mL L^{-1} failing to create hypoxic or anoxic conditions defined by oxygen concentrations below 2 mL L^{-1} . UL-CWCs (*E. dabneyi*, *P. josephinae* and *D. aff. meteor*) only occurred above the oxygen minimum and were associated to a very narrow thermal range (Figure D.9 a-c), with most predicted suitable habitat occurring at seafloor temperatures comprised between 10 and $12 \text{ }^\circ\text{C}$ (Figs. 8e and 10a). UIL-CWCs (*V. flagellum*, *C. verticillata* and *Acanthogorgia* spp.) mostly occurred above and within the oxygen minimum zone. They appeared to tolerate most of the environmental conditions occurring in the upper 800 m of the water column (Fig. 10b). IDL-CWCs (*D. pertusum*, *M. oculata* and *L. expansa*) mostly occurred below and within the oxygen minimum zone and their predicted suitable habitat was almost entirely associated with seafloor location characterized by near-constant background values of nutrient concentrations

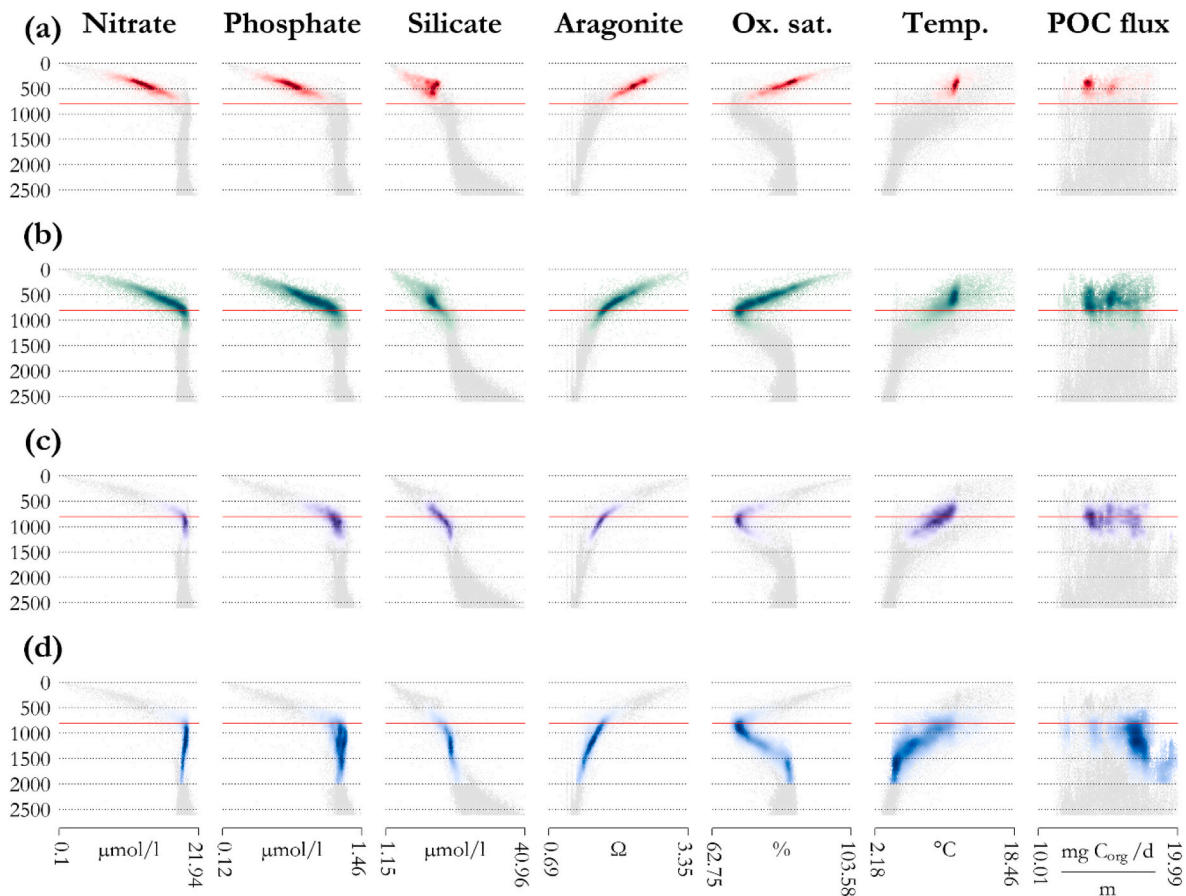


Fig. 10. Environmental values associated to high-confidence suitable cells plotted against depth (m). Plots of aragonite and calcite saturation levels had a very similar profile, thus only aragonite is shown. The red line marks the minimum concentration of oxygen in the region ($\sim 4.28 \text{ ml l}^{-1}$ at 805 m). High-confidence suitable cells are combined into four groups: (a) upper layer cold-water corals (UL-CWCs): *Errina dabneyi*, *Paracalyptophora josephinae* and *Dentomuricea aff. meteor*; (b) upper-intermediate layer cold-water corals (UIL-CWCs) in green: *Viminella flagellum*, *Callogorgia verticillata* and *Acanthogorgia* spp.; (c) intermediate layer cold-water corals (IL-CWCs) in purple: *Narella bellissima*, *Narella versluysi*, *Coralliidae* spp., and *Paragorgia johnsoni*; (d) intermediate-deep layer cold-water corals (IDL-CWCs) in blue: *Desmophyllum pertusum*, *Madrepora oculata* and *Leiopathes cf. expansa*. The darker the colour, the denser are the suitable cells within a specific plot region. In grey, the regional background values. Seafloor areas below 2000 m depth were not modelled. Ox. Sat.: oxygen saturation; Temp.: temperature; POC: particulate organic carbon.

(Figs. 8c and 10d).

3.5. Niche overlap

The pair-wise niche overlap and the results of niche equivalence and niche similarity tests are shown in Fig. 11. IL-CWCs (*N. bellissima*, *N. versluysi*, *Coralliidae* spp. and *P. johnsoni*) showed the highest degree of niche overlap and were significantly more similar among themselves than expected by random chance, yet their niches were not equivalent. UIL-CWCs (*V. flagellum*, *C. verticillata* and *Acanthogorgia* spp.) presented equivalent niches, i.e. statistically not more different from each other than expected by random chance given the regional environmental conditions. This suggests that most of the latitudinal and longitudinal changes observed in their estimated distribution are due to terrain variables, which were not used to compute the niche space. Considering UL-CWCs, the niches of *E. dabneyi* and *D. aff. meteor* were equivalent. In addition, the niches of *P. josephinae* and *D. aff. meteor* were equivalent to the niche of *C. verticillata* (UIL-CWC). The niches of UL- and UIL-CWCs Schoener's D overlap values between 0.4 and 0.6 (1 being the maximum) suggesting that these species can co-exist in certain areas. *E. dabneyi* and *Acanthogorgia* spp. had the niches that showed the lowest overlap with other UL- and UIL-CWCs niches. *D. pertusum* and *M. oculata* (IDL-CWCs) occupied an equivalent niche space and showed a very low niche overlap with UL- and UIL-CWCs and a low overlap with IL-CWCs.

L. cf. expansa (IDL-CWCs) presented a higher degree of overlap with IL-CWCs than *D. pertusum* and *M. oculata*. However most of the similarity tests between *L. cf. expansa* and the taxa of the intermediate layer were not significant when keeping the occurrence values of *L. cf. expansa* while shifting the position of IL-CWCs.

4. Discussion

4.1. Distributions

Our models suggest that almost all major elevations and island complexes host habitats that are suitable for the studied CWCs, particularly areas located on the Mid-Atlantic Ridge (MAR), the Central and Southeastern Seamounts and the island slopes. These taxa seemed to exist on both sides of the MAR and at most latitudes, which is in line with the results of previous studies (Braga-Henriques et al., 2013). The only exception was *Errina dabneyi*, which largely concentrated in central Azores. Wide latitudinal and longitudinal ranges of CWCs have been reported in previous studies performed in regions that have extensions similar to our study area (e.g. Barbosa et al., 2020; Georgian et al., 2019) and, in general, wide geographic distributions seem to be a characteristic common to many deep-sea species (McClain and Rex, 2015). The concentration of suitable areas east of the MAR and at latitudes delimited by the northern and southern-most islands (Corvo and Santa

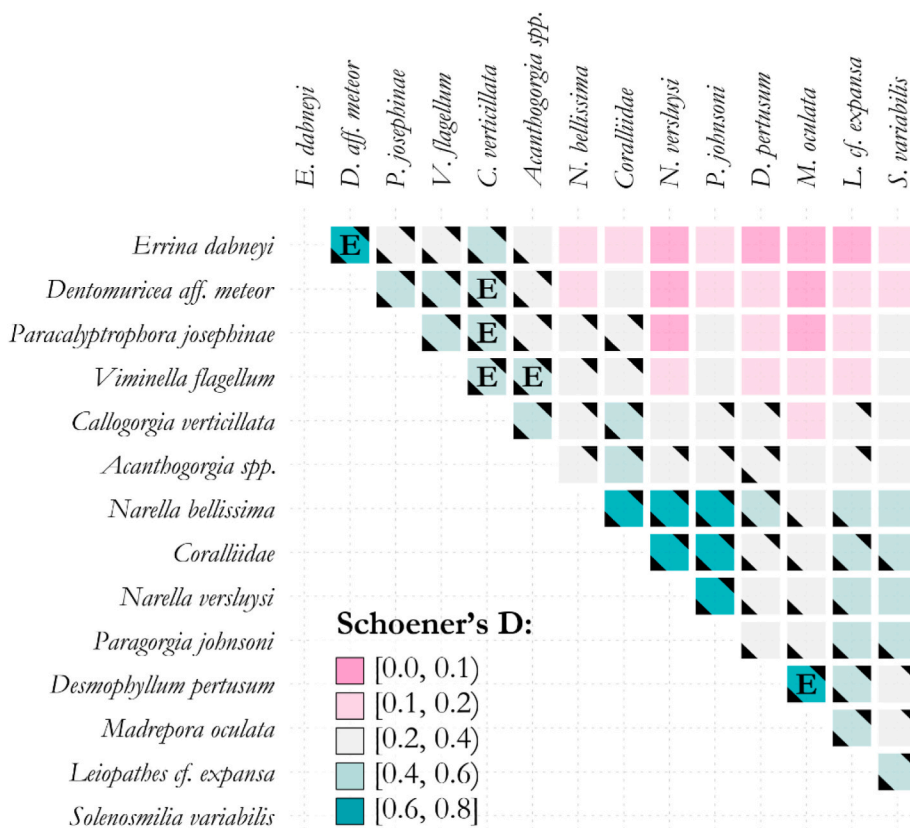


Fig. 11. Niche overlap computed from the predictors 'seawater chemistry', particulate organic carbon flux, temperature, oxygen saturation and current speed. Only high-confidence suitable cells were considered for the computation of the niches. The letter 'E' identifies pairs of taxa whose niches were not significantly different from each other (equivalent niches) ($\alpha > 0.05$). The black triangles identify pairs of species whose niches were significantly ($P < 0.05$) more similar than expected by chance. Triangles in the bottom-left corners identify significant similarity tests of the row species when random shifting of the spatial distribution of the column species. Triangles in the upper-right corners identify significant similarity tests of the column species when random shifting of the spatial distribution of the row species.

Maria, respectively) is probably owed to the abundance of shallow elevations at these latitudes.

Model predictions seem to confirm that the considered CWCs depend on hard substrates for their settlement and development. In fact, suitable habitats for these taxa were mostly found on complex topographic features and were virtually absent from flat and low relief areas (areas generally characterized by soft sediments). Hard substrates and complex topographic features have long been known to be important drivers of habitat-forming CWC distribution (Roberts et al., 2009). In our 1 km² grid cells, these properties were captured by the covariates slope and bathymetric position index (BPI 5 km and BPI 20 km) with the species modelled avoiding slopes below 5° and BPI values close to zero. At this resolution, steepness and relative elevation were taken as proxies for seafloor complexity, occurrence of rocky substrate and topographically-driven current acceleration, which are abiotic variables that more directly influence CWC occurrence (Baco et al., 2020; Henry et al., 2013; Juva et al., 2020; Levin et al., 2010; Mohn et al., 2014; Morato et al., 2021b). The difficulty in building accurate regional maps for these seafloor variables from sparse data explains the low explanatory power they generally have at broad scales (e.g. Bennecke and Metaxas, 2017; Georgian et al., 2019). Nonetheless, resolving the patchiness of surficial sediment types and habitat complexity will be most relevant to improve the predictive power or future model addressing finer scales. As our video annotation suggests, continuous rocky patches rarely cover entire 1 km² patches.

Different primary production regimes exist in the region, with the Azores Current-Azores Front system delimiting different circulation and production regimes (Amorim et al., 2017; Caldeira and Reis, 2017; Frazão et al., 2022). More productive waters are typically located north of the archipelago while less productive waters are found to the south of it. Although food export from the surface is a major factor shaping deep-sea benthic communities (Woolley et al., 2016), the variable POC flux did not show a clear pattern in our models. It was a shared important variable (i.e. important both for GAM and Maxent models) for

Desmophyllum pertusum, *Madrepora oculata* and *Leiopathes cf. expansa*, driving their estimated distribution toward high productivity sectors of the northern MAR. However, habitat suitable for these species was also found in the southern part of the study area. A second possibility is that enhanced carbon fluxes allow these species to inhabit deeper waters in the northern part of the study area, where most of their preferential habitat is located. The control of food availability over tolerance ranges and coral fitness has been pointed out in previous studies (Flögel et al., 2014; Hanz et al., 2019; Hebbeln et al., 2020).

In general, all the considered taxa had patches of suitable habitat in the central portion of the study area. On the contrary, the Southern Seamounts and the slopes around Santa Maria, located in less productive waters, appeared suitable for fewer modelled species. This suggests that the latitudinal gradient in productivity could generate a gradual turnover of species, with moderate changes in the composition of benthic assemblages over large latitudinal gradients already identified as a common pattern in the deep sea (e.g. Bridges et al., 2021; McClain and Rex, 2015). Caldeira and Reis (2017) found that the eastern group of islands and the Southern Seamounts are strongly influenced by the Azores Current and by its westward-propagating eddies, while the remaining portion of the study area is under the influence of the Gulf Stream. Silva et al. (2013) found a north-south gradient in the composition of phytoplanktonic species. These findings support the idea that a regional latitudinal gradient in species composition sustained by environmental factors could influence deep-sea benthic communities. Future studies that consider population densities rather than simple presence data, coupled with new explanatory variables better incorporating the pelagic-benthic coupling and hydrodynamic regimes, will be necessary to confirm the existence of this gradient in the region.

4.2. Species pools

The bathymetric zonation of the modelled species was strong, with a clear species turnover along the depth gradient. This reflects a well-

documented pattern in literature (e.g. Brandt et al., 2019; Victorero et al., 2018) and reiterates the narrow vertical extent and fast depth-wise turnover in the Azores coral facies suggested by Tempera et al. (2012) and Braga-Henriques et al. (2013). Interestingly, model predictions suggest that the vertical turnover of species is organized around the regional oxygen minimum and is associated to the stratification of water masses.

The poor explanatory value oxygen saturation showed in most models contrasts with the value it seems to have for interpreting their outputs. The reason for this probably relates to the way oxygen saturation varies along the bathymetric gradient. Correlative models associate the presence of a species to particular values of a predictor variable, and the fact that oxygen saturation and dissolved oxygen concentrations assume similar values above and below the oxygen minimum at very different depths, likely becomes a confounding factor for correlative models. Thus, indirect predictors not affected by similar problems can emerge as better explanatory variables. In all our models, 'seawater chemistry' was by far the most important predictor. The grouping of dissolved nutrient concentrations with variables describing seawater carbonate chemistry to serve as a proxy of the water mass vertical zonation in the region is unconventional. In fact, these variables have different physiological effects on CWCs. The saturation states of aragonite and calcite are critical parameters for the biomineralization of skeletal structures (Conci et al., 2021; Tambutté et al., 2011) and their importance as predictor variables was evident in studies modelling the distribution of coral species at global or basin scales (Davies and Guinotte, 2011; Morato et al., 2020c; Yesson et al., 2012). However, the carbonate saturation horizons in the study area occur at greater depths than those modelled. Therefore, while the saturation states of aragonite and calcite can still play a role in determining the suitability of particular locations and the vertical turnover of species, it is unlikely that they represent the only factors explaining the observed depth zonation. Similarly, dissolved nutrients influence the physiology of CWCs (Goldberg, 2018). However, to our knowledge, there is no study identifying the concentration of water nutrient as a key explanatory variable of CWC distributions.

The variable 'seawater chemistry' seems to successfully seize the vertical stratification of the regional water masses. When considering its individual components in relation to depth, we remark that the concentration of nutrients increases from shallow waters down to a certain depth and then stabilizes. The depth at which this inflection occurs corresponds to the depth of the regional minimum concentration of dissolved oxygen and to the depth where the core of intermediate waters is located (ca. 800 m). Model predictions are structured around these patterns.

A water mass can be considered an environmental envelop characterized by a particular combination of oceanographic parameters (Emery, 2001; Liu and Tanhua, 2021) that influences carbonate equilibria and food supply (Azetsu-Scott et al., 2010; Emery, 2001; Fontela et al., 2020; González-Dávila et al., 2011). The effects of water masses on the depth zonation of deep biota is supported by several studies and it is likely caused by multiple processes such as promotion or hampering of dispersal, environmental filtering, spatial segregation, speciation and physical phenomena altering the food supply (e.g. internal waves) (Carney, 2005; Puerta et al., 2020; Quattrini et al., 2017; Radice et al., 2016; Roberts et al., 2021; Victorero et al., 2018). These processes likely produce biodiversity and biogeographic patterns, even over local scales of several hundred meters (Carney, 2005; Puerta et al., 2020). In the Azores, Puerta et al. (2022) found that the regional stratification of the water column was useful to explain the vertical distribution of deep-sea megabenthic assemblages, while Menezes et al. (2006) found that water-mass boundaries and oxygen content influenced the zonation of demersal fish assemblages. In line with these studies, our models suggest that the stratification of regional water masses play a critical role in the zonation of deep biota and, in particular, of habitat-forming CWCs. One group of corals was strongly associated to the intermediate layer

(IL-CWCs) and a second group strongly associated with the upper layer (UL-CWCs). The other groups of CWCs (UIL- and IDL-CWCs) seemed to be limited to upper and intermediate or deep and intermediate layers. This suggests that water masses can act either as a strong or a soft environmental filter depending on the species. Rephrasing Carney (2005) and his study on the zonation of deep biota on continental margins, these pools of CWCs seem to represent species truly restricted to upper water masses, species extending down from upper water masses, species truly restricted to intermediate water masses and species extending up from deep water masses. The projection of model predictions into the niche space, which is less prone to geographic biases in habitat availability (Brown and Carnaval, 2019), produced similar results.

In this perspective, regional intermediate waters and their boundaries represent interesting areas where to explore patterns of α and β diversity of CWC assemblages. In fact, intermediate waters seem to host a distinctive group of species but, at the same time, they seem to act as a transition zone for shallow and deep coral species, pretty much like the transition zones described by Carney (2005). While recent analyses provide a preliminary support to this idea (Arantes et al., 2009; Auscavitch et al., 2020; Puerta et al., 2022; Serrano et al., 2017), the investigation of this hypothesis represents an interesting topic for future studies.

4.3. Management implications

Despite the topographic richness that characterises the Azores region, the combined habitat of all modelled species covered only 11% of the study area. Although apparently modest, the suitable habitat held by the Azores seamounts, islands and Mid-Atlantic Ridge segments are likely at the core of the metapopulation dynamics sustaining viable CWC populations over a broad ocean basin dominated by abyssal plains (Addamo et al., 2021; Boavida et al., 2019). As Mironov and Krylova (2006) have previously suggested, the Azores might represent a centre of redistribution of marine fauna, i.e. an area where organisms having different geographical origins intermix, with obvious implications for international conservation strategies at ocean basin scale (Badgley et al., 2017; Combes et al., 2021; Dunn et al., 2018). Special concern deserves *Errina dabneyi*. This species has an extremely limited range and seems to be endemic to the Azores (Braga-Henriques et al., 2011; Zibrowius and Cairns, 1992). Active conservation actions to favour its long-term conservation should be considered a priority (Costello and Chaudhary, 2017).

Nevertheless, all the modelled species should be viewed as important targets for conservation. In fact, they all possess the characteristics of engineer species (Crotty et al., 2019; Ellison, 2019) and represent indicator taxa of vulnerable marine ecosystems (FAO, 2009). Therefore, they are of great importance both for ecological research and regional spatial management. Acting as foundation species, these taxa can be expected to play a key role in ecological facilitation and, thus, in the structuring of deep-sea benthic communities (Kikvidze and Callaway, 2009). Being part of vulnerable marine ecosystems they are, by definition, affected by anthropogenic disturbance (Clark and Tittensor, 2010; Ragnarsson et al., 2017). In the light of their limited projected habitat and the pressures they face in the region, spatial protection is advised for these species. Documented threats include a sustained fishing pressure extending to remote fishing grounds (Morato et al., 2021b) and attested by the sizeable amounts of lost fishing gears observed in recent surveys (Dominguez-Carrió, unpublished data). At decadal scales, forecasted changes in water chemistry in the deep sea due to climate change (Sweetman et al., 2017) is yet another threat to benthic species, with consequences expected to be particularly severe at mid latitudes including the Azores (Levin et al., 2020; Morato et al., 2020c). Emerging plans for deep-sea mining would further increase threats to the deep-sea organisms in the region (Carreiro-Silva et al., 2022; Lopes et al., 2019; Martins et al., 2022; Morato et al., 2022).

If spatial closures were to be implemented in the area following representativity criteria (Stevens, 2002), these networks should ideally cover all the vertical layers in which regional water masses are stratified. Given the marked vertical zonation of the modelled CWCs, steep seafloor elevations intersecting the different water masses (e.g. Gigante Seamount Complex) constitute prime targets for conservation (McClain and Rex, 2015) as they concentrate distinct faunal assemblages over short distances. Although our models provided only limited evidence of the two ecological regions demarcated by the Azores Front-Azores Current system (Caldeira and Reis, 2017; Frazão et al., 2022) and their distinct production regimes, this information should be considered in the design of networks of marine protected areas based on the precautionary approach.

Note that suitable habitats were identified after a robust and thorough evaluation of the quality of model predictions based on indexes measuring performance and similarity of model outputs. A robust model evaluation is essential to inform management strategies and support ecological investigation (Araújo et al., 2019) and represent a strength of the proposed combined habitat suitability maps which place great emphasis in the identification of ‘high-confidence’ zones, i.e. zones considered the safest to make inferences about CWCs distributions.

4.4. Performance, caveats and plausibility

Presence-only models are generally affected by important limitations, therefore, it is challenging to draw general conclusions based on their predictions (Bowden et al., 2021). In our case, a major drawback relies on the lack of high-resolution layers derived from oceanographic models that integrate tidal effects over topographic structures. In fact, while communities dwelling below the photic layer rely on food that sinks through the water column, the strength of the pelagic–benthic coupling depends on fluctuating seabed currents (e.g. Jansen et al., 2018; Juva et al., 2020; Mohn et al., 2014). The layer of near-bottom current computed by VIKING20 (Böning et al., 2016) and used in this study did not consider tidal effects and, hence, showed limited utility as a predictor variable. Another drawback is linked to the bathymetric grid used, which derives from multibeam and non-multibeam data (EMODnet, 2018). The lack of fine-scale information in areas that currently do not have multibeam data (e.g. Kurchatov Fracture Zone) likely led to erroneous predictions. Besides the depth-derived layers, the coarse native resolution of the remaining environmental layers further limited the capacity of HSMs to discriminate between suitable and unsuitable areas. These limitations seemed more evident when assessing the latitudinal and longitudinal distribution of model predictions. On the contrary, HSMs seemed able to capture the major bathymetric patterns existing in the region. Community composition and environmental conditions show a greater change over depth than over latitude (McClain and Rex, 2015; Quattrini et al., 2017; Victorero et al., 2018), a variability likely better captured by the layers available and, as consequence, by our models.

According to traditional performance indicators (AUC and TSS), GAM and Maxent models had good or fair performance. However, discriminatory scores alone have a limited utility in evaluating presence-only models without the use of independent datasets. Thus, the ecological plausibility of model predictions and other measures of model uncertainty should be taken into account (Araújo et al., 2019; Warren et al., 2020). Uncertainties arising from alternative model structures and from biases in the response variables were addressed by employing a bootstrap and a fuzzy matching process. The overall similarity of model predictions was measured considering improved Fuzzy Kappa scores (F_{kHC} and F_k). Models agreed better in areas where suitability predictions were less affected by the resampling of the input data ($F_{kHC} > F_k$). Until new information becomes available, these ‘high-confidence’ zones should be considered the safest to make inferences about CWCs distributions. Part of the noise in model predictions appeared to be caused by bycatch records. In fact, areas where bycatch records were the

main source of information (e.g. Princess Alice and Açor) were associated to habitat suitability predictions with low or medium confidence levels, indicating that video records should be regarded as much better sources of information for these type of analyses.

Efforts should be made to increase the number of occurrence records available to fit HSMs because it seemed to influence the quality and the similarity of model predictions. Nevertheless, most models seemed to produce ecologically sound predictions. This was the case for octocoral and *Errina dabneyi* models, which produced habitat suitability maps that were in line with the distributional patterns emerging from regional surveys (e.g. Morato et al., 2021b, 2020b, 2019b). Model predictions for stony and black corals (i.e. *Desmophyllum pertusum*, *Madrepora oculata*, *Solenosmilia variabilis* and *Leiopathes cf. expansa*) appeared less robust, with habitat suitability maps capturing reasonably well the upper depth limit of their distributions but potentially over-predicting their geographic distribution relative to field observations. These coral taxa inhabit the deepest portion of the modelled area and, with the exception of *Solenosmilia variabilis*, comprise the IDL-CWC group. The sampling effort below 1500 m depth was scarce, therefore, all results concerning IDL-CWCs should be considered cautiously as the proposed models could fail in correctly detecting the lower depth limit of their distributions and some of their environmental responses. Nevertheless, we believe that sufficient data was available to correctly identify their minimum depth of occurrence, which appears to be in line with the distributional patterns emerging from regional surveys (e.g. Morato et al., 2021b, 2020b, 2019b). Additionally, the lack of environmental predictors that accurately link surface productivity, current regimes and food availability at the seafloor could be particularly relevant for IDL-CWCs models. In fact, the supply of organic matter mediated by flow dynamics is known to be a key factor for the development of deep-sea stony corals (Fink et al., 2015; Hebbeln et al., 2020; Juva et al., 2020; Raddatz et al., 2020) and for black coral species of the genus *Leiopathes* (Lim et al., 2020). In particular, areas presenting similar geomorphic and environmental settings but different food inputs could not be discriminated by the proposed models, likely causing a problem of over-prediction. This over-prediction can be expected to be more severe for species associated with the deepest portion of the study area, since chemical energy gains increasing relevance in shaping the distribution of deep-sea organisms as we move away from surface waters (McClain and Rex, 2015; Woolley et al., 2016).

5. Conclusions

Our results show that over the considered bathymetric range (0–2000 m), CWCs form four groups of species: species restricted to upper water masses, species extending down from upper water masses, species restricted to intermediate water masses and species extending up from deep water masses. Such depth zonation is most likely determined by the vertical stratification of regional water masses. Our results also provide some preliminary evidence about the possible influence of the different production regimes determined Azores Front-Azores Current system on the distribution of CWC taxa in the Azores. The geographic and bathymetric patterns identified have important implications for the spatial management of all the modelled CWCs which represent foundation species and are expected to influence, directly or indirectly, their associated biota. The Azores is one of a few regions off the Atlantic margins that encompass topographic features high enough to intersect water masses from abyssal depths to the upper ocean. It represents a hotspot of suitable habitat for the modelled CWC taxa and is likely an area of basin-wide relevance for maintaining interconnected populations of CWCs and concentrate conservation initiatives. Despite the topographic richness that characterises the Azores region, the combined habitat of all modelled species covered only 11% of the study area. Being foundation organisms and indicator taxa of vulnerable marine ecosystems and because of the small seafloor area they cover, spatial protection is advised for all the modelled CWC taxa.

Declaration of competing interest

The authors declare that they have no known competing financial interests or personal relationships that could have appeared to influence the work reported in this paper

Data availability

All model outputs have been made available for download on the data repository PANGAEA.

Acknowledgments

This work contributes to the PO2020 MapGES (Acores-01-0145-FEDER-000056) research project and to the European Union's Horizon 2020 research and innovation programme under grant agreement No 678760 (ATLAS), No 818123 (iAtlantic) and No 824077 (EURO-FLEETS+). This output reflects only the authors' views and the European Union cannot be held responsible for any use that may be made of the information contained therein. We acknowledge all projects and programs that collected occurrence data of cold-water coral species in the Azores region. Records in the COLETA database were originally collected by fisheries observer programs during the CORAZON project (FCT No PTDC/MAR/72169/2006), HERMIONE project (FP7 No 226354) and CoralFISH (FP7 GA 213144) harbour sampling programs; CoralFISH, DiscardLess (H2020 No 633680), MERCES (H2020 No 689518) and SPONGES (H2020 No 679849). Records were also provided by the fisheries survey programs ARQDAÇO (1995–2019), OASIS (FP7 No EVK3-CT-2002-00073), CoralFISH, CONDOR (EEA grants No PT0040/2008), PESCPROF (Interreg IIB/MAC/4.2/M12), DEECON (FCT EURODEEP/0002/2007) and BIOMETORE (EEA grants No PT02), and by the FISHOR experimental bottom trawl surveys. Finally, occurrence records were also made available by multiple ROV, submersible and towed video surveys such as those conducted within the MapGES, BIOMETORE, Estrutura de Missão para Extensão da Plataforma Continental (EMEP; Cruzeiro Científico EMEPC/LUSO/Açores/2009), MEDWAVES (ATLAS No 678760, with logistic and technical assistance from the UTM-CSIC and the financial support from the Spanish Ministry of Economy, Industry and Competitiveness), Blue Azores 2018 (National Geographic Pristine Seas program, Oceano Azul Foundation, and Waitt Institute), NICO 12 Expedition and Pelagia Rainbow 2019 (64PE441, 64PE454, and 64PE456; Netherlands Organisation for Scientific Research NWO for funding and Royal Netherlands Institute for Sea Research NIOZ for organising the Netherlands Initiative Changing Oceans NICO expedition in 2018), TREASURE (RV Pelagia cruises 64PE388, 64PE398, 64PE412, NWO-TTW grant 13273 and Topsector Water), and iMAR 2021 (RV Pelagia ship-time was provided free of charge as part of the iMAR project which received funding from the European Union's H2020 Research & Innovation Programme under grant agreement No 824077 EURO-FLEETS+). We deeply thank all fisheries observers, PIs, crews and scientists that participated in all these sampling programs. GHT was supported by the DRCT (M3.1. a/F/052/2015). TM was supported by Program Investigador FCT (IF/01194/2013), and the IFCT Exploratory Project (IF/01194/2013/CP1199/CT0002) from the Fundação para a Ciência e Tecnologia (POPH and QREN). TM and MCS were also supported by the FCT-IP Program Stimulus of Scientific Employment (CCCIND/03345/2020 and CCCIND/03346/2020, respectively) and the H2020 programme No 689518 (MERCES) and No 818123 (iAtlantic). CD-C was supported by the PO2020 projects MapGES and DeepWalls (Acores-01-0145-FEDER-000056 and Acores-01-0145-FEDER-000124) and by the FCT-IP Project UIDP/05634/2020. CKP received support from the Operational Program Azores 2020, through the Fund 01-0145-FEDER-000140 "MarAZ Researchers: Consolidate a body of researchers in Marine Sciences in the Azores" of the European Union. We also acknowledge funds through the FCT – Foundation for Science and Technology, I.P., under the project

OKEANOS UIDB/05634/2020 and UIDP/05634/2020 and through the FCT Regional Government of the Azores under the project M1.1. A/REEQ.CIENTÍFICO UI&D/2021/010.

Appendix A. Supplementary data

Supplementary data to this article can be found online at <https://doi.org/10.1016/j.dsr.2023.104028>.

References

- Addamo, A.M., Miller, K.J., Häussermann, V., Taviani, M., Machordom, A., 2021. Global-scale genetic structure of a cosmopolitan cold-water coral species. *Aquat. Conserv. Mar. Freshw. Ecosyst.* 31, 1–14. <https://doi.org/10.1002/aqc.3421>.
- Allouche, O., Tsoar, A., Kadmon, R., 2006. Assessing the accuracy of species distribution models: prevalence, kappa and the true skill statistic (TSS). *J. Appl. Ecol.* 43, 1223–1232. <https://doi.org/10.1111/j.1365-2664.2006.01214.x>.
- Amorim, P., Perán, A.D., Pham, C.K., Juliano, M., Cardigos, F., Tempera, F., Morato, T., 2017. Overview of the ocean climatology and its variability in the azores region of the North Atlantic including environmental characteristics at the seabed. *Front. Mar. Sci.* 4, 1–16. <https://doi.org/10.3389/fmars.2017.00056>.
- Arantes, R., Castro, C., Pires, D., Seoane, J., 2009. Depth and water mass zonation and species associations of cold-water octocoral and stony coral communities in the southwestern Atlantic. *Mar. Ecol. Prog. Ser.* 397, 71–79. <https://doi.org/10.3354/meps08230>.
- Araújo, M.B., Anderson, R.P., Márcia Barbosa, A., Beale, C.M., Dormann, C.F., Early, R., Garcia, R.A., Guisan, A., Maiorano, L., Naimi, B., O'Hara, R.B., Zimmermann, N.E., Rahbek, C., 2019. Standards for distribution models in biodiversity assessments. *Sci. Adv.* 5, eaat4858 <https://doi.org/10.1126/sciadv.aat4858>.
- Armstrong, C.W., Aanesen, M., Rensburg, T.M., Sandorf, E.D., 2019. Willingness to pay to protect cold water corals. *Conserv. Biol.*, 13380 <https://doi.org/10.1111/cobi.13380>, 0, cob1.
- Auscavitch, S.R., Deere, M.C., Keller, A.G., Rotjan, R.D., Shank, T.M., Cordes, E.E., 2020. Oceanographic drivers of deep-sea coral species distribution and community assembly on seamounts, islands, atolls, and reefs within the Phoenix Islands Protected Area. *Front. Mar. Sci.* 7, 1–15. <https://doi.org/10.3389/fmars.2020.00042>.
- Azetsu-Scott, K., Clarke, A., Falkner, K., Hamilton, J., Jones, E.P., Lee, C., Petrie, B., Prinsenberg, S., Starr, M., Yeats, P., 2010. Calcium carbonate saturation states in the waters of the Canadian Arctic archipelago and the Labrador Sea. *J. Geophys. Res.* 115, C11021 <https://doi.org/10.1029/2009JC005917>.
- Baco, A.R., Morgan, N.B., Roark, E.B., 2020. Observations of vulnerable marine ecosystems and significant adverse impacts on high seas seamounts of the northwestern Hawaiian Ridge and Emperor Seamount Chain. *Mar. Pol.* 115, 103834 <https://doi.org/10.1016/j.marpol.2020.103834>.
- Badgley, C., Smiley, T.M., Terry, R., Davis, E.B., DeSantis, L.R.G., Fox, D.L., Hopkins, S.S.B., Jezkova, T., Matocq, M.D., Matzke, N., McGuire, J.L., Mulch, A., Riddle, B.R., Roth, V.L., Samuels, J.X., Strömberg, C.A.E., Yanites, B.J., 2017. Biodiversity and topographic complexity: modern and geohistorical perspectives. *Trends Ecol. Evol.* 32, 211–226. <https://doi.org/10.1016/j.tree.2016.12.010>.
- Barbet-Massin, M., Jiguet, F., Albert, C.H., Thuiller, W., 2012. Selecting pseudo-absences for species distribution models: how, where and how many? *Methods Ecol. Evol.* 3, 327–338. <https://doi.org/10.1111/j.2041-210X.2011.00172.x>.
- Barbosa, R.V., Davies, A.J., Sumida, P.Y.G., 2020. Habitat suitability and environmental niche comparison of cold-water coral species along the Brazilian continental margin. *Deep-Sea Res. Part I Oceanogr. Res. Pap.* 155, 103147 <https://doi.org/10.1016/j.dsr.2019.103147>.
- Bartoň, K., 2022. MuMin: Multi-Model Inference. R Package Version 1.46.0.
- Bashmachnikov, I., Nascimento, Neves, F., Menezes, T., Koldunov, N.V., 2015. Distribution of intermediate water masses in the subtropical northeast Atlantic. *Ocean Sci.* 11, 803–827. <https://doi.org/10.5194/os-11-803-2015>.
- Bennecke, S., Metaxas, A., 2017. Is substrate composition a suitable predictor for deep-water coral occurrence on fine scales? *Deep-Sea Res. Part I Oceanogr. Res. Pap.* 124, 55–65. <https://doi.org/10.1016/j.dsr.2017.04.011>.
- Boavida, J., Becheler, R., Choquet, M., Frank, N., Taviani, M., Bourillet, J., Meistertzheim, A., Grehan, A., Savini, A., Arnaud-Haond, S., 2019. Out of the Mediterranean? Post-glacial colonization pathways varied among cold-water coral species. *J. Biogeogr.* 46, 915–931. <https://doi.org/10.1111/jbi.13570>.
- Böning, C.W., Behrens, E., Biastoch, A., Getzlaff, K., Bamber, J.L., 2016. Emerging impact of Greenland meltwater on deepwater formation in the North Atlantic Ocean. *Nat. Geosci.* 9, 523–527. <https://doi.org/10.1038/ngeo2740>.
- Bowden, D.A., Anderson, O.F., Rowden, A.A., Stephenson, F., Clark, M.R., 2021. Assessing habitat suitability models for the deep sea: is our ability to predict the distributions of seafloor fauna improving? *Front. Mar. Sci.* 8 <https://doi.org/10.3389/fmars.2021.632389>.
- Braga-Henriques, A., Carreiro-Silva, M., Porteiro, F.M., de Matos, V., Sampaio, I., Ocaña, O., Ávila, S.P., 2011. The association between a deep-sea gastropod *Pedicularia sicula* (Caenogastropoda: pediculariidae) and its coral host *Errina dabneyi* (Hydrozoa: Stylasteridae) in the Azores. *ICES J. Mar. Sci.* 68, 399–407. <https://doi.org/10.1093/icesjms/fsq066>.
- Braga-Henriques, A., Porteiro, F.M., Ribeiro, P.A., de Matos, V., Sampaio, I., Ocaña, O., Santos, R.S., 2013. Diversity, distribution and spatial structure of the cold-water

- coral fauna of the Azores (NE Atlantic). *Biogeosciences* 10, 4009–4036. <https://doi.org/10.5194/bg-10-4009-2013>.
- Brandt, A., Alaluykina, I., Brix, S., Brenke, N., Błażewicz, M., Golovan, O.A., Johannsen, N., Hrinko, A.M., Jazdzewski, A.M., Jeskulke, K., Kamenev, G.M., Lavrenteva, A.V., Malyutina, M.V., Riehl, T., Lins, L., 2019. Depth zonation of Northwest Pacific deep-sea macrofauna. *Prog. Oceanogr.* 176, 102131 <https://doi.org/10.1016/j.pocean.2019.102131>.
- Bridges, A.E.H., Barnes, D.K.A., Bell, J.B., Ross, R.E., Howell, K.L., 2021. Benthic assemblage composition of South Atlantic seamounts. *Front. Mar. Sci.* 8, 1–18. <https://doi.org/10.3389/fmars.2021.660648>.
- Brown, J.L., Carnaval, A.C., 2019. A tale of two niches: methods, concepts, and evolution. *Front. Biogeogr.* 11 <https://doi.org/10.21245/F5FBG44158>.
- Buhl-Mortensen, L., Vanreusel, A., Gooday, A.J., Levin, L.A., Priede, I.G., Buhl-Mortensen, P., Gheerardyn, H., King, N.J., Raes, M., 2010. Biological structures as a source of habitat heterogeneity and biodiversity on the deep ocean margins. *Mar. Ecol. Prog. Ser.* 321, 21–50. <https://doi.org/10.1111/j.1439-0485.2010.00359.x>.
- Buhl-Mortensen, P., Buhl-Mortensen, L., Purser, A., 2017. Trophic ecology and habitat provision in cold-water coral ecosystems. In: Rossi, S., Bramanti, L., Gori, A., Orejas, C. (Eds.), *Marine Animal Forests*. Springer International Publishing, Cham, pp. 1–42. https://doi.org/10.1007/978-3-319-17001-5_17-2.
- Cadotte, M.W., Tucker, C.M., 2017. Should environmental filtering be abandoned? *Trends Ecol. Evol.* 32, 429–437. <https://doi.org/10.1016/j.tree.2017.03.004>.
- Cairns, S.D., 2007. Deep-water corals: an overview with special reference to diversity and distribution of deep-water scleractinian corals. *Bull. Mar. Sci.* 81, 311–322.
- Caldeira, R.M.A., Reis, J.C., 2017. The azores confluence zone. *Front. Mar. Sci.* 4, 1–14. <https://doi.org/10.3389/fmars.2017.00037>.
- Carney, R., 2005. Zonation of deep biota on continental margins. In: *Oceanography and Marine Biology*, pp. 211–278. <https://doi.org/10.1201/9781420037449.ch6>.
- Carreiro-Silva, M., Andrews, A., Braga-Henriques, A., de Matos, V., Porteiro, F., Santos, R., 2013. Variability in growth rates of long-lived black coral *Leiopathes* sp. from the Azores. *Mar. Ecol. Prog. Ser.* 473, 189–199. <https://doi.org/10.3354/meps10052>.
- Carreiro-Silva, M., Martins, A., Sampaio, I., Loureiro, C.M., Gonçalves, A., Mendes, C., Morato, T., 2015. Cruise report BIOMETORE 2015 to the great meteor complex seamounts (Atlantis and Irving) onboard the NRP almirante gago coutinho. Zenodo. <https://doi.org/10.5281/zenodo.7433209>.
- Carreiro-Silva, M., Martins, I., Riou, V., Raimundo, J., Caetano, M., Bettencourt, R., Rakka, M., Cerqueira, T., Godinho, A., Morato, T., Colaço, A., 2022. Mechanical and toxicological effects of deep-sea mining sediment plumes on a habitat-forming cold-water octocoral. *Front. Mar. Sci.* 9, 1–23. <https://doi.org/10.3389/fmars.2022.915650>.
- Carreiro-Silva, M., Ramos, M., Morato, T., 2019. Greenpeace Pole-to-Pole expedition – azores 2019. Zenodo. <https://doi.org/10.5281/zenodo.6557865>.
- Cathalot, C., Van Oevelen, D., Cox, T.J.S., Kutti, T., Lavaleye, M., Duineveld, G., Meysman, F.J.R., 2015. Cold-water coral reefs and adjacent sponge grounds: hotspots of benthic respiration and organic carbon cycling in the deep sea. *Front. Mar. Sci.* 2, 1–12. <https://doi.org/10.3389/fmars.2015.00037>.
- Clark, M.R., Titterson, D.P., 2010. An index to assess the risk to stony corals from bottom trawling on seamounts. *Mar. Ecol. Prog. Ser.* 310, 200–211. <https://doi.org/10.1111/j.1439-0485.2010.00392.x>.
- Combes, M., Vaz, S., Grehan, A., Morato, T., Arnaud-Haond, S., Dominguez-Carrió, C., Fox, A., González-Irusta, J.M., Johnson, D., Callery, O., Davies, A., Fauconnet, L., Kenchington, E., Orejas, C., Roberts, J.M., Taranto, G., Menot, L., 2021. Systematic conservation planning at an ocean basin scale: identifying a viable network of deep-sea protected areas in the North Atlantic and the Mediterranean. *Front. Mar. Sci.* 8, 1–27. <https://doi.org/10.3389/fmars.2021.611358>.
- Conci, N., Vargas, S., Wörheide, G., 2021. The biology and evolution of calcite and aragonite mineralization in octocorallia. *Front. Ecol. Evol.* 9, 1–19. <https://doi.org/10.3389/fevo.2021.623774>.
- Cornell, H.V., Harrison, S.P., 2014. What are species pools and when are they important? *Annu. Rev. Ecol. Evol. Syst.* 45, 45–67. <https://doi.org/10.1146/annurev-ecolsys-120213-091759>.
- Costello, M.J., Chaudhary, C., 2017. Marine biodiversity, biogeography, deep-sea gradients, and conservation. *Curr. Biol.* 27, R511–R527. <https://doi.org/10.1016/j.cub.2017.04.060>.
- Crotty, S.M., Altieri, A.H., Bruno, J.F., Fischman, H., Bertness, M.D., 2019. The foundation for building the conservation capacity of community ecology. *Front. Mar. Sci.* 6, 1–8. <https://doi.org/10.3389/fmars.2019.00238>.
- Cyr, F., Haren, H., Mienis, F., Duineveld, G., Bourgault, D., 2016. On the influence of cold-water coral mound size on flow hydrodynamics, and vice versa. *Geophys. Res. Lett.* 43, 775–783. <https://doi.org/10.1002/2015GL067038>.
- D'Amen, M., Rahbek, C., Zimmermann, N.E., Guisan, A., 2017. Spatial predictions at the community level: from current approaches to future frameworks. *Biol. Rev.* 92, 169–187. <https://doi.org/10.1111/brv.12222>.
- D'Onghia, G., 2019. Cold-water corals as shelter, feeding and life-history critical habitats for fish species: ecological interactions and fishing impact. In: Orejas, C., Jiménez, C. (Eds.), *Mediterranean Cold-Water Corals: Past, Present and Future*. Springer International Publishing, Cham, pp. 335–356. https://doi.org/10.1007/978-3-319-91608-8_30.
- Davies, A.J., Guinotte, J.M., 2011. Global habitat suitability for framework-forming cold-water corals. *PLoS One* 6, e18483. <https://doi.org/10.1371/journal.pone.0018483>.
- Demšar, U., Harris, P., Brunson, C., Fotheringham, A.S., McLoone, S., 2013. Principal component analysis on spatial data: an overview. *Ann. Assoc. Am. Geogr.* 103, 106–128. <https://doi.org/10.1080/00045608.2012.689236>.
- Dominguez-Carrió, C., Gollner, S., Morato, T., 2019a. RV Pelagia cruise 64PE454: Rainbow hydrothermal vent and southern MAR 2019, Hopper tow-cam video footage. Zenodo. <https://doi.org/10.5281/zenodo.6593981>.
- Dominguez-Carrió, C., Gollner, S., Visser, F., Morato, T., 2019b. Cruise report - NICO cruise leg 12, hopper dives on board of R/V Pelagia. Zenodo. <https://doi.org/10.5281/zenodo.3416992>.
- Dominguez-Carrió, C., Fontes, J., Morato, T., 2021. A cost-effective video system for a rapid appraisal of deep-sea benthic habitats: the Azor drift-cam. *Methods Ecol. Evol.* 12, 1379–1388. <https://doi.org/10.1111/2041-210X.13617>.
- Dormann, C.F., Elith, J., Bacher, S., Buchmann, C., Carl, G., Carré, G., Marquéz, J.R.G., Gruber, B., Lafourcade, B., Leitão, P.J., Münkemüller, T., McClean, C., Osborne, P.E., Reineking, B., Schröder, B., Skidmore, A.K., Zurell, D., Lautenbach, S., 2013. Collinearity: a review of methods to deal with it and simulation study evaluating their performance. *Ecography* 36, 27–46. <https://doi.org/10.1111/j.1600-0587.2012.07348.x>.
- Dormann, C.F., McPherson, J.M., Araújo, M.B., Bivand, R., Bolliger, J., Carl, G., Davies, R.G., Hirzel, A., Jetz, W., Daniel Kissling, W., Kühn, I., Ohlemüller, R., Peres-Neto, P.R., Reineking, B., Schröder, B., Schurr, F.M., Wilson, R., 2007. Methods to account for spatial autocorrelation in the analysis of species distributional data: a review. *Ecography* 30, 609–628. <https://doi.org/10.1111/j.2007.0906-7590.05171.x>.
- Drake, J.M., Randin, C., Guisan, A., 2006. Modelling ecological niches with support vector machines. *J. Appl. Ecol.* 43, 424–432. <https://doi.org/10.1111/j.1365-2664.2006.01141.x>.
- Duineveld, G., 2017. Cruise report - REPORT PELAGIA CRUISE 64PE412 TREASURE (towards responsible ExtrAction of Submarine REsources) horta - horta 25 June – 13 July 2016. Zenodo. <https://doi.org/10.5281/zenodo.556556>.
- Dunn, D.C., Van Dover, C.L., Etter, R.J., Smith, C.R., Levin, L.A., Morato, T., Colaço, A., Dale, A.C., Gebruk, A.V., Gjerde, K.M., Halpin, P.N., Howell, K.L., Johnson, D., Perez, J.A.A., Ribeiro, M.C., Stuckas, H., Weaver, P., 2018. A strategy for the conservation of biodiversity on mid-ocean ridges from deep-sea mining. *Sci. Adv.* 4, 1–16. <https://doi.org/10.1126/sciadv.aar4313>.
- Elith, J., Ferrier, S., Huettmann, F., Leathwick, J., 2005. The evaluation strip: a new and robust method for plotting predicted responses from species distribution models. *Ecol. Model.* 186, 280–289. <https://doi.org/10.1016/j.ecolmodel.2004.12.007>.
- Elith, J., Leathwick, J.R., 2009. Species distribution models: ecological explanation and prediction across space and time. *Annu. Rev. Ecol. Evol. Syst.* 40, 677–697. <https://doi.org/10.1146/annurev.ecolsys.110308.120159>.
- Ellison, A.M., 2019. Foundation species, non-trophic interactions, and the value of being common. *iScience* 13, 254–268. <https://doi.org/10.1016/j.isci.2019.02.020>.
- Emery, W.J., 2001. Water types and water masses. In: *Encyclopedia of Ocean Sciences*. Elsevier, pp. 3179–3187. <https://doi.org/10.1006/rwos.2001.0108>.
- EMODnet, 2018. EMODnet digital bathymetry (DTM 2018). <https://doi.org/10.1277/0/18ff0d48-b203-4a65-94a9-5fd8b0ec35f6>.
- FAO, 2009. *International Guidelines for the Management of Deep-Sea Fisheries in the High Seas*. FAO, Rome.
- Fink, H.G., Wienberg, C., De Pol-Holz, R., Hebbeln, D., 2015. Spatio-temporal distribution patterns of Mediterranean cold-water corals (*Lophelia pertusa* and *Madrepora oculata*) during the past 14,000 years. *Deep-Sea Res. Part 1 Oceanogr. Res. Pap.* 103, 37–48. <https://doi.org/10.1016/j.jdsr.2015.05.006>.
- Flögel, S., Dullo, W.C., Pfannkuche, O., Kiriakoulakis, K., Rüggeberg, A., 2014. Geochemical and physical constraints for the occurrence of living cold-water corals. *Deep. Res. Part II Top. Stud. Oceanogr.* 99, 19–26. <https://doi.org/10.1016/j.dsr2.2013.06.006>.
- Fontela, M., Pérez, F.F., Carracedo, L.I., Padín, X.A., Velo, A., García-Ibañez, M.I., Lherminier, P., 2020. The Northeast Atlantic is running out of excess carbonate in the horizon of cold-water corals communities. *Sci. Rep.* 10, 14714 <https://doi.org/10.1038/s41598-020-71793-2>.
- Frazão, H.C., Prien, R.D., Schulz-Bull, D.E., Seidov, D., Waniek, J.J., 2022. The forgotten azores current: a long-term perspective. *Front. Mar. Sci.* 9, 1–14. <https://doi.org/10.3389/fmars.2022.842251>.
- Georgian, S.E., Anderson, O.F., Rowden, A.A., 2019. Ensemble habitat suitability modeling of vulnerable marine ecosystem indicator taxa to inform deep-sea fisheries management in the South Pacific Ocean. *Fish. Res.* 211, 256–274. <https://doi.org/10.1016/j.fishres.2018.11.020>.
- Georgian, S.E., Deleó, D., Durkin, A., Gomez, C.E., Kurman, M., Lunden, J.J., Cordes, E. E., 2016. Oceanographic patterns and carbonate chemistry in the vicinity of cold-water coral reefs in the Gulf of Mexico: implications for resilience in a changing ocean. *Limnol. Oceanogr.* 61, 648–665. <https://doi.org/10.1002/lno.10242>.
- Goldberg, W.M., 2018. Coral food, feeding, nutrition, and secretion: a review. In: Kloc, M., Kubiak, J.Z. (Eds.), *Marine Organisms as Model Systems in Biology and Medicine, Results and Problems in Cell Differentiation*, 65. Springer, Cham, pp. 377–421. https://doi.org/10.1007/978-3-319-92486-1_18.
- Gomes-Pereira, J.N., Carmo, V., Catarino, D., Jakobsen, J., Alvarez, H., Aguilar, R., Hart, J., Giacomello, E., Menezes, G., Stefanni, S., Colaço, A., Morato, T., Santos, R. S., Tempera, F., Porteiro, F., 2017. Cold-water corals and large hydrozoans provide essential fish habitat for *Lappanella fasciata* and *Benthocometes robustus*. *Deep. Res. Part II Top. Stud. Oceanogr.* 145, 33–48. <https://doi.org/10.1016/j.dsr2.2017.09.015>.
- González-Dávila, M., Santana-Casiano, J.M., Fine, R.A., Happell, J., Delille, B., Speich, S., 2011. Carbonate system in the water masses of the southeast Atlantic sector of the southern ocean during february and march 2008. *Biogeosciences* 8, 1401–1413. <https://doi.org/10.5194/bg-8-1401-2011>.
- Hagen-Zanker, A., 2009. An improved Fuzzy Kappa statistic that accounts for spatial autocorrelation. *Int. J. Geogr. Inf. Sci.* 23, 61–73. <https://doi.org/10.1080/13658810802570317>.

- Hagen, A., 2003. Fuzzy set approach to assessing similarity of categorical maps. *Int. J. Geogr. Inf. Sci.* 17, 235–249. <https://doi.org/10.1080/13658810210157822>.
- Hanz, U., Wienberg, C., Hebbeln, D., Duineveld, G., Lavaley, M., Juva, K., Dullo, W.-C., Freiwald, A., Tamborrino, L., Reichart, G.-J., Flögel, S., Mienis, F., 2019. Environmental factors influencing benthic communities in the oxygen minimum zones on the Angolan and Namibian margins. *Biogeosciences* 16, 4337–4356. <https://doi.org/10.5194/bg-16-4337-2019>.
- Hastie, T., Tibshirani, R., 1990. *Generalized Additive Models*. Chapman & Hall/CRC, New York/Boca Raton.
- Hebbeln, D., Wienberg, C., Dullo, W.-C., Freiwald, A., Mienis, F., Orejas, C., Titschack, J., 2020. Cold-water coral reefs thriving under hypoxia. *Coral Reefs*. <https://doi.org/10.1007/s00338-020-01934-6>.
- Henry, L.-A., Moreno Navas, J., Roberts, J.M., 2013. Multi-scale interactions between local hydrography, seabed topography, and community assembly on cold-water coral reefs. *Biogeosciences* 10, 2737–2746. <https://doi.org/10.5194/bg-10-2737-2013>.
- Hijmans, R., Phillips, S.J., Leathwick, J., Elith, J., 2022. *Dismo: Species Distribution Modeling*, pp. 3–5. R package version 1.
- Hortal, J., De Bello, F., Diniz-Filho, J.A.F., Lewinsohn, T.M., Lobo, J.M., Ladle, R.J., 2015. Seven shortfalls that beset large-scale knowledge of biodiversity. *Annu. Rev. Ecol. Syst.* 46, 523–549. <https://doi.org/10.1146/annurev-ecolsys-112414-054400>.
- Iturbide, M., Bedia, J., Gutiérrez, J.M., 2018. Tackling uncertainties of species distribution model projections with package mopa. *R J* 10, 122. <https://doi.org/10.32614/RJ-2018-019>.
- Jansen, J., Hill, N.A., Dunstan, P.K., McKinlay, J., Sumner, M.D., Post, A.L., Eléaume, M. P., Armand, L.K., Warnock, J.P., Galton-Fenzi, B.K., Johnson, C.R., 2018. Abundance and richness of key Antarctic seafloor fauna correlates with modelled food availability. *Nat. Ecol. Evol.* 2, 71–80. <https://doi.org/10.1038/s41559-017-0392-3>.
- Johnson, J., Stevens, I., 2000. A fine resolution model of the Eastern North Atlantic between the azores, the canary islands and the Gibraltar strait. *Deep-Sea Res. Part I Oceanogr. Res. Pap.* 47, 875–899. [https://doi.org/10.1016/S0967-0637\(99\)00073-4](https://doi.org/10.1016/S0967-0637(99)00073-4).
- Juva, K., Flögel, S., Karstensen, J., Linke, P., Dullo, W.-C., 2020. Tidal dynamics control on cold-water coral growth: a high-resolution multivariable study on eastern atlantic cold-water coral sites. *Front. Mar. Sci.* 7, 1–23. <https://doi.org/10.3389/fmars.2020.00132>.
- Kikvidze, Z., Callaway, R.M., 2009. Ecological facilitation may drive major evolutionary transitions. *Bioscience* 59, 399–404. <https://doi.org/10.1525/bio.2009.59.5.7>.
- Klompmaier, A.A., Jakobsen, S.L., Lauridsen, B.W., 2016. Evolution of body size, vision, and biodiversity of coral-associated organisms: evidence from fossil crustaceans in cold-water coral and tropical coral ecosystems. *BMC Evol. Biol.* 16, 132. <https://doi.org/10.1186/s12862-016-0694-0>.
- Kraft, N.J.B., Adler, P.B., Godoy, O., James, E.C., Fuller, S., Levine, J.M., 2015. Community assembly, coexistence and the environmental filtering metaphor. *Funct. Ecol.* 592–599. <https://doi.org/10.1111/1365-2435.12345>.
- Landis, J.R., Koch, G.G., 1977. The measurement of observer agreement for categorical data. *Biometrics* 33, 159. <https://doi.org/10.2307/2529310>.
- Lecours, V., Dolan, M.F.J., Micallef, A., Lucier, V.L., 2016. A review of marine geomorphometry, the quantitative study of the seafloor. *Hydrol. Earth Syst. Sci.* 20, 3207–3244. <https://doi.org/10.5194/hess-20-3207-2016>.
- Levin, L.A., Sibuet, M., Gooday, A.J., Smith, C.R., Vanreusel, A., 2010. The roles of habitat heterogeneity in generating and maintaining biodiversity on continental margins: an introduction. *Mar. Ecol.* 31, 1–5. <https://doi.org/10.1111/j.1439-0485.2009.00358.x>.
- Levin, L.A., Wei, C., Dunn, D.C., Amon, D.J., Ashford, O.S., Cheung, W.W.L., Colaço, A., Dominguez-Carrió, C., Escobar, E.G., Harden-Davies, H.R., Drazen, J.C., Ismail, K., Jones, D.O.B., Johnson, D.E., Le, J.T., Lejzerowicz, F., Mitarai, S., Morato, T., Mulsow, S., Snelgrove, P.V.R., Sweetman, A.K., Yasuhara, M., 2020. Climate change considerations are fundamental to management of deep-sea resource extraction. *Global Change Biol.* 26, 4664–4678. <https://doi.org/10.1111/gcb.15223>.
- Lim, A., Wheeler, A.J., Price, D.M., O'Reilly, L., Harris, K., Conti, L., 2020. Influence of benthic currents on cold-water coral habitats: a combined benthic monitoring and 3D photogrammetric investigation. *Sci. Rep.* 10, 19433. <https://doi.org/10.1038/s41598-020-76446-y>.
- Linley, T.D., Lavaley, M., Maiorano, P., Bergman, M., Capezzuto, F., Cousins, N.J., D'Onghia, G., Duineveld, G., Shields, M.A., Sion, L., Tursi, A., Priede, I.G., 2017. Effects of cold-water corals on fish diversity and density (European continental margin: arctic, NE Atlantic and Mediterranean Sea): data from three baited lander systems. *Deep Sea Res. Part II Top. Stud. Oceanogr.* 145, 8–21. <https://doi.org/10.1016/j.dsr2.2015.12.003>.
- Liu, C., Berry, P.M., Dawson, T.P., Pearson, R.G., 2005. Selecting thresholds of occurrence in the prediction of species distributions. *Ecography* 28, 385–393. <https://doi.org/10.1111/j.0966-7590.2005.03957.x>.
- Liu, M., Tanhua, T., 2021. Water masses in the Atlantic Ocean: characteristics and distributions. *Ocean Sci.* 17, 463–486. <https://doi.org/10.5194/os-17-463-2021>.
- Lopes, C.L., Bastos, L., Caetano, M., Martins, I., Santos, M.M., Iglesias, I., 2019. Development of physical modelling tools in support of risk scenarios: a new framework focused on deep-sea mining. *Sci. Total Environ.* 650, 2294–2306. <https://doi.org/10.1016/j.scitotenv.2018.09.351>.
- Lundblad, E.R., Wright, D.J., Miller, J., Larkin, E.M., Rinehart, R., Naar, D.F., Donahue, B.T., Anderson, S.M., Battista, T., 2006. A benthic terrain classification scheme for American Samoa. *Mar. Geodes.* 29, 89–111. <https://doi.org/10.1080/01490410600738021>.
- Lutz, M.J., Caldeira, K., Dunbar, R.B., Behrenfeld, M.J., 2007. Seasonal rhythms of net primary production and particulate organic carbon flux to depth describe the efficiency of biological pump in the global ocean. *J. Geophys. Res.* 112, C10011. <https://doi.org/10.1029/2006JC003706>.
- Martins, I., Godinho, A., Rakka, M., Carreiro-Silva, M., 2022. Beyond deep-sea mining sublethal effects: delayed mortality from acute Cu exposure of the cold-water octocoral *Viminella flagellum*. *Mar. Pollut. Bull.* 183, 114051. <https://doi.org/10.1016/j.marpolbul.2022.114051>.
- McClain, C.R., Rex, M.A., 2015. Toward a conceptual understanding of β -diversity in the deep-sea benthos. *Annu. Rev. Ecol. Syst.* 46, 623–642. <https://doi.org/10.1146/annurev-ecolsys-120213-091640>.
- Menezes, G., Sigler, M., Silva, H., Pinho, M., 2006. Structure and zonation of demersal fish assemblages off the Azores Archipelago (mid-Atlantic). *Mar. Ecol. Prog. Ser.* 324, 241–260. <https://doi.org/10.3354/meps324241>.
- Middelburg, J.J., Mueller, C.E., Veuger, B., Larsson, A.I., Form, A.U., Oevelen, D. van, 2016. Discovery of symbiotic nitrogen fixation and chemoautotrophy in cold-water corals. *Sci. Rep.* 5, 17962. <https://doi.org/10.1038/srep17962>.
- Mienis, F., Bouma, T., Witbaard, R., van Oevelen, D., Duineveld, G., 2019. Experimental assessment of the effects of cold-water coral patches on water flow. *Mar. Ecol. Prog. Ser.* 609, 101–117. <https://doi.org/10.3354/meps12815>.
- Mironov, A.N., Krylova, E.M., 2006. Origin of the fauna of the meteor seamounts, north-eastern atlantic. In: Mironov, Alexander N., Southward, A.J., Gebbruk, A.V. (Eds.), *Biogeography of the North Atlantic Seamounts*. KMK Scientific Press, pp. 22–57.
- Mitchell, N.C., Stretch, R., Tempera, F., Ligi, M., 2018. Volcanism in the Azores: a marine geophysical perspective. *Act. Volcanoes World* 101–126. https://doi.org/10.1007/978-3-642-32226-6_7.
- Mohn, C., Rengstorf, A., White, M., Duineveld, G., Mienis, F., Soetaert, K., Grehan, A., 2014. Linking benthic hydrodynamics and cold-water coral occurrences: a high-resolution model study at three cold-water coral provinces in the NE Atlantic. *Prog. Oceanogr.* 122, 92–104. <https://doi.org/10.1016/j.poccean.2013.12.003>.
- Morato, T., Carreiro-Silva, M., Dominguez-Carrió, C., Taranto, G.H., Rodrigues, L., Brito, J., Gomes, S., 2019a. Cruise report - MapGES/ATLAS project: august 2018 cruise on board of R/V arquipélago. Zenodo. <https://doi.org/10.5281/zenodo.3417022>.
- Morato, T., Carreiro-Silva, M., Taranto, G.H., Dominguez-Carrió, C., Ramos, M., Ríos, N., Fauconnet, L., Ocaña Vicente, O., Calado, A., Afonso, A., Ramos, B., Souto, M., Bettencourt, R., 2019b. Cruise report - blue azores program expedition 2018 on board the nrp gago coutinho. Zenodo. <https://doi.org/10.5281/zenodo.3416898>.
- Morato, T., Dominguez-Carrió, C., Evans, S., Taranto, G.H., Neves de Sousa, L., Mohn, C., Carreiro-Silva, M., 2021a. iMAR: integrated assessment of the distribution of vulnerable marine ecosystem along the Mid-Atlantic Ridge in the azores region. Zenodo. <https://doi.org/10.5281/zenodo.6556837>.
- Morato, T., Dominguez-Carrió, C., Gomes, S., Taranto, G.H., Ramos, M., Fauconnet, L., Rodrigues, L., Carreiro-Silva, M., 2020a. MapGES 2020 Cruise Report: Exploration of Azores Deep-Sea Habitats summer 2020.
- Morato, T., Dominguez-Carrió, C., Gomes, S., Taranto, G.H., Blasco-Ferre, J., Ramos, M., Fauconnet, L., Zarate, C., Carreiro-Silva, M., 2020b. MapGES 2019: summer 2019 cruise on board of N/I arquipélago. Zenodo. <https://doi.org/10.5281/zenodo.3727570>.
- Morato, T., Dominguez-Carrió, C., Mohn, C., Ocaña Vicente, O., Ramos, M., Rodrigues, L., Sampaio, I., Taranto, G.H., Fauconnet, L., Tojeira, I., Gonçalves, E.J., Carreiro-Silva, M., 2021b. Dense cold-water coral garden of *Paragorgia johnsoni* suggests the importance of the Mid-Atlantic Ridge for deep-sea biodiversity. *Ecol. Evol.* 11, 16426–16433. <https://doi.org/10.1002/ece3.8319>.
- Morato, T., González-Irusta, J., Dominguez-Carrió, C., Wei, C., Davies, A., Sweetman, A. K., Taranto, G.H., Beazley, L., Garcia-Alegre, A., Grehan, A., Laffargue, P., Murrillo, F. J., Sacau, M., Vaz, S., Kenchington, E., Arnaud-Haond, S., Callery, O., Chimienti, G., Cordes, E., Egilsdottir, H., Freiwald, A., Gasbarro, R., Gutiérrez-Zarate, C., Gianni, M., Gilkinson, K., Wareham Hayes, V.E., Hebbeln, D., Hedges, K., Henry, L., Johnson, D., Koen-Alonso, M., Lurette, C., Mastrototaro, F., Menot, L., Molodtsova, T., Durán Muñoz, P., Orejas, C., Pennino, M.G., Puerta, P., Ragnarsson, S.Á., Ramiro-Sánchez, B., Rice, J., Riverá, J., Roberts, J.M., Ross, S.W., Rueda, J.L., Sampaio, I., Snelgrove, P., Stirling, D., Treble, M.A., Urra, J., Vad, J., Oevelen, D., Watling, L., Walkusz, W., Wienberg, C., Woillez, M., Levin, L.A., Carreiro-Silva, M., 2020c. Climate-induced changes in the suitable habitat of cold-water corals and commercially important deep-sea fishes in the North Atlantic. *Glob. Change Biol.* gcb, 14996. <https://doi.org/10.1111/gcb.14996>.
- Morato, T., Juliano, M., Pham, C.K., Carreiro-Silva, M., Martins, I., Colaço, A., 2022. Modelling the dispersion of seafloor massive sulphide mining plumes in the mid Atlantic Ridge around the azores. *Front. Mar. Sci.* 9, 1–18. <https://doi.org/10.3389/fmars.2022.910940>.
- Orejas, C., Addamo, A., Alvarez, M., Aparicio, A., Alcoverro, D., Arnaud-Haond, S., Bilan, M., Boavida, J., Cainzos, V., Calderon, R., Cambeiro, P., Castano, M., Fox, A., Gallardo, M., Gori, A., Gutierrez, C., Henry, L.-A., Hermdia, M., Jimenez, J.A., Lopez-Jurado, J.L., Lozano, P., Mateo-Ramirez, A., Mateu, G., Matoso, J.L., Mendez, C., Morillas, A., Movilla, J., Olariaga, A., Paredes, M., Pelayo, V., Pineiro, S., Rakka, M., Ramirez, T., Ramos, M., Reis, J., Riverá, J., Romero, A., Rueda, J.L., Salvador, T., Sampaio, I., Sanchez, H., Santiago, R., Serrano, A., Taranto, G., Urra, J., Velez-Belchi, P., Viladrich, N., Zein, M., 2017. Cruise summary report - MEDWAVES survey (Mediterranean out flow Water and vulnerable Ecosystems). Zenodo. <https://doi.org/10.5281/zenodo.556516>.
- Orejas, C., Jiménez, C., 2017. The builders of the oceans - Part I: coral architecture from the tropics to the Poles, from the shallow to the deep. In: Rossi, S., Bramanti, L., Gori, A., Orejas, C. (Eds.), *Marine Animal Forests*. Springer International Publishing, Cham, pp. 627–655. https://doi.org/10.1007/978-3-319-21012-4_10.
- Paradis, E., Schliep, K., 2019. Ape 5.0: an environment for modern phylogenetics and evolutionary analyses in R. *Bioinformatics* 35, 526–528. <https://doi.org/10.1093/bioinformatics/bty633>.

- Peran, A.D., Pham, C.K., Amorim, P., Cardigos, F., Tempera, F., Morato, T., 2016. Seafloor characteristics in the azores region (North Atlantic). *Front. Mar. Sci.* 3, 2014–2017. <https://doi.org/10.3389/fmars.2016.00204>.
- Phillips, S.J., Anderson, R.P., Schapire, R.E., 2006. Maximum entropy modeling of species geographic distributions. *Ecol. Model.* 190, 231–259. <https://doi.org/10.1016/j.ecolmodel.2005.03.026>.
- Phillips, S.J., Dudík, M., Elith, J., Graham, C.H., Lehmann, A., Leathwick, J., Ferrier, S., 2009. Sample selection bias and presence-only distribution models: implications for background and pseudo-absence data. *Ecol. Appl.* 19, 181–197. <https://doi.org/10.1890/07-2153.1>.
- Puerta, P., Johnson, C., Carreiro-Silva, M., Henry, L.-A., Kenchington, E., Morato, T., Kazanidis, G., Rueda, J.L., Urrea, J., Ross, S., Wei, C.-L., González-Irusta, J.M., Arnaud-Haond, S., Orejas, C., 2020. Influence of water masses on the biodiversity and biogeography of deep-sea benthic ecosystems in the North Atlantic. *Front. Mar. Sci.* 7, 1–25. <https://doi.org/10.3389/fmars.2020.00239>.
- Puerta, P., Mosquera-Giménez, A., Reñones, O., Domínguez-Carrió, C., Rueda, J.L., Urrea, J., Carreiro-Silva, M., Blasco-Ferre, J., Santana, Y., Gutiérrez-Zárate, C., Véllez-Belchí, P., Rivera, J., Morato, T., Orejas, C., 2022. Variability of deep-sea megabenthic assemblages along the western pathway of the Mediterranean outflow water. *Deep-Sea Res. Part I Oceanogr. Res. Pap.* 185, 103791. <https://doi.org/10.1016/j.dsr.2022.103791>.
- Quattrini, A.M., Gómez, C.E., Cordes, E.E., 2017. Environmental filtering and neutral processes shape octocoral community assembly in the deep sea. *Oecologia* 183, 221–236. <https://doi.org/10.1007/s00442-016-3765-4>.
- R Core Team, 2022. *R: A Language and Environment for Statistical Computing*.
- Raddatz, J., Titschack, J., Frank, N., Freiwald, A., Conforti, A., Osborne, A., Skornitzke, S., Stiller, W., Rüggeberg, A., Voigt, S., Albuquerque, A.L.S., Vertino, A., Schröder-Ritzrau, A., Bahr, A., 2020. *Solenosmilia variabilis*-bearing cold-water coral mounds off Brazil. *Coral Reefs, Coral Reefs of the World* 39, 69–83. <https://doi.org/10.1007/s00338-019-01882-w>.
- Radice, V.Z., Quattrini, A.M., Wareham, V.E., Edinger, E.N., Cordes, E.E., 2016. Vertical water mass structure in the North Atlantic influences the bathymetric distribution of species in the deep-sea coral genus *Paramuricea*. *Deep-Sea Res. Part I Oceanogr. Res. Pap.* 116, 253–263. <https://doi.org/10.1016/j.dsr.2016.08.014>.
- Ragnarsson, S.A., Burgos, J.M., Kutti, T., Beld, I. Van Den, Egilsdóttir, H., Arnaud-Haond, S., Grehan, A., 2017. The Impact of Anthropogenic Activity on Cold-Water Corals, Marine Animal Forests. Springer International Publishing, Cham. <https://doi.org/10.1007/978-3-319-17001-5>.
- Rix, L., De Goeij, J.M., Mueller, C.E., Struck, U., Middelburg, J.J., Van Duyl, F.C., Al-Horani, F.A., Wild, C., Naumann, M.S., Van Oevelen, D., 2016. Coral mucus fuels the sponge loop in warm- and cold-water coral reef ecosystems. *Sci. Rep.* 6, 1–11. <https://doi.org/10.1038/srep18715>.
- Roberts, E., Bowers, D., Meyer, H., Samuelsen, A., Rapp, H., Cárdenas, P., 2021. Water masses constrain the distribution of deep-sea sponges in the North Atlantic Ocean and nordic seas. *Mar. Ecol. Prog. Ser.* 659, 75–96. <https://doi.org/10.3354/meps13570>.
- Roberts, J.M., Cairns, S.D., 2014. Cold-water corals in a changing ocean. *Curr. Opin. Environ. Sustain.* 7, 118–126. <https://doi.org/10.1016/j.cosust.2014.01.004>.
- Roberts, J.M., Wheeler, A., Freiwald, A., Cairns, S.D., 2009. *Cold-Water Corals*. Cambridge University Press, Cambridge. <https://doi.org/10.1017/CBO9780511581588>.
- Rovelli, L., Attard, K., Bryant, L., Flögel, S., Stahl, H., Roberts, J.M., Linke, P., Glud, R., 2015. Benthic O₂ uptake of two cold-water coral communities estimated with the non-invasive eddy correlation technique. *Mar. Ecol. Prog. Ser.* 525, 97–104. <https://doi.org/10.3354/meps11211>.
- Rovelli, L., Carreiro-Silva, M., Attard, K., Rakka, M., Domínguez-Carrió, C., Bilan, M., Blackburn, S., Morato, T., Wolff, G., Glud, R., 2022. Benthic O₂ uptake by coral gardens at the Condor seamount (Azores). *Mar. Ecol. Prog. Ser.* 688, 19–31. <https://doi.org/10.3354/meps14021>.
- Sala, I., Harrison, C.S., Caldeira, R.M.A., 2016. The role of the Azores Archipelago in capturing and retaining incoming particles. *J. Mar. Syst.* 154, 146–156. <https://doi.org/10.1016/j.jmarsys.2015.10.001>.
- Sampaio, I., Braga-Henriques, A., Pham, C., Ocaña, O., de Matos, V., Morato, T., Porteiro, F.M., 2012. Cold-water corals landed by bottom longline fisheries in the Azores (north-eastern Atlantic). *J. Mar. Biol. Assoc. U. K.* 92, 1547–1555. <https://doi.org/10.1017/S0025315412000045>.
- Sampaio, I., Freiwald, A., Porteiro, F.M., Menezes, G., Carreiro-Silva, M., 2019a. Census of octocorallia (cnidaria: anthozoa) of the azores (NE Atlantic) with a nomenclature update. *Zootaxa* 4550, 451–498. <https://doi.org/10.11646/zootaxa.4550.4.1>.
- Sampaio, I., Morato, T., Porteiro, F., Gutiérrez-Zárate, C., Taranto, G., Pham, C., Gonçalves, J., Carreiro-Silva, M., 2019b. The value of a deep-sea collection of the azores (NE Atlantic Ocean): marine invertebrate biodiversity in an era of global environmental change. *Biodivers. Inf. Sci. Stand.* 3. <https://doi.org/10.3897/biss.3.37209>.
- Schölkopf, B., Platt, J.C., Shawe-Taylor, J., Smola, A.J., Williamson, R.C., 2001. Estimating the support of a high-dimensional distribution. *Neural Comput.* 13, 1443–1471. <https://doi.org/10.1162/089976601750264965>.
- Serrano, A., Cartes, J.E., Papiol, V., Punzón, A., García-Alegre, A., Arronte, J.C., Ríos, P., Lourido, A., Frutos, I., Blanco, M., 2017. Epibenthic communities of sedimentary habitats in a NE Atlantic deep seamount (Galicia Bank). *J. Sea Res.* 130, 154–165. <https://doi.org/10.1016/j.seares.2017.03.004>.
- Silva, A., Brotas, V., Valente, A., Sá, C., Diniz, T., Patarra, R.F., Álvaro, N.V., Neto, A.I., 2013. Coccolithophore species as indicators of surface oceanographic conditions in the vicinity of Azores islands. *Estuar. Coast Shelf Sci.* 118, 50–59. <https://doi.org/10.1016/j.ecss.2012.12.010>.
- Soetaert, K., Mohn, C., Rengstorf, A., Grehan, A., van Oevelen, D., 2016. Ecosystem engineering creates a direct nutritional link between 600-m deep cold-water coral mounds and surface productivity. *Sci. Rep.* 6, 35057. <https://doi.org/10.1038/srep35057>.
- Somoza, L., Medialdea, T., González, F.J., Calado, A., Afonso, A., Albuquerque, M., Asensio-Ramos, M., Bettencourt, R., Blasco, I., Candón, J.A., Carreiro-Silva, M., Cid, C., De Ignacio, C., López-Pamo, E., Machancoses, S., Ramos, B., Ribeiro, L.P., Rincón-Tomás, B., Santofimia, E., Souto, M., Tojeira, I., Viegas, C., Madureira, P., 2020. Multidisciplinary scientific cruise to the northern Mid-Atlantic Ridge and azores archipelago. *Front. Mar. Sci.* 7, 1–9. <https://doi.org/10.3389/fmars.2020.568035>.
- Stevens, T., 2002. Rigor and representativeness in marine protected area design. *Coast. Manag.* 30, 237–248. <https://doi.org/10.1080/08920750290042183>.
- Sweetman, A.K., Thurber, A.R., Smith, C.R., Levin, L.A., Mora, C., Wei, C.-L., Gooday, A. J., Jones, D.O.B., Rex, M., Yasuhara, M., Ingels, J., Ruhl, H.A., Frieder, C.A., Danovaro, R., Würzberg, L., Baco, A.R., Grube, B.M., Pasulka, A., Meyer, K.S., Dunlop, K.M., Henry, L.-A., Roberts, J.M., 2017. Major impacts of climate change on deep-sea benthic ecosystems. *Elem. Sci. Anth* 5, 4. <https://doi.org/10.1525/elementa.203>.
- Symonds, M.R.E., Moussalli, A., 2011. A brief guide to model selection, multimodel inference and model averaging in behavioural ecology using Akaike's information criterion. *Behav. Ecol. Sociobiol.* 65, 13–21. <https://doi.org/10.1007/s00265-010-1037-6>.
- Tambutté, S., Holcomb, M., Ferrier-Pagès, C., Reynaud, S., Tambutté, E., Zoccola, D., Allemand, D., 2011. Coral biomineralization: from the gene to the environment. *J. Exp. Mar. Biol. Ecol.* 408, 58–78. <https://doi.org/10.1016/j.jembe.2011.07.026>.
- Taranto, G.H., González-Irusta, J., Domínguez-Carrió, C., Pham, C.K., Tempera, F., Ramos, M., Gonçalves, G., Carreiro-Silva, M., Morato, T., 2023. Habitat suitability maps for vulnerable and foundation cold-water coral taxa of the Azores (NE Atlantic). *Pangea*. <https://doi.org/10.1594/PANGAEA.955223>.
- Tempera, F., Pereira, J., Braga-Henriques, A., Porteiro, F.M., Morato, T., de Matos, V., Souto, M., Guillaumont, B., Santos, R.S., 2012. Cataloguing deep-sea biological faunas of the Azores. *Rev. Investig. Mar.* 19, 36–38.
- Thuiller, W., Georges, D., Gueguen, M., Engler, R., Breiner, F., Lafourcade, B., 2022. *biomod2: Ensemble Platform for Species Distribution Modeling*. R package version 4.0.
- Thuiller, W., Lafourcade, B., Engler, R., Araújo, M.B., 2009. *Biomod - a platform for ensemble forecasting of species distributions*. *Ecography* 32, 369–373. <https://doi.org/10.1111/j.1600-0587.2008.05742.x>.
- Thurber, A.R., Sweetman, A.K., Narayanaswamy, B.E., Jones, D.O.B., Ingels, J., Hansman, R.L., 2014. Ecosystem function and services provided by the deep sea. *Biogeosciences* 11, 3941–3963. <https://doi.org/10.5194/bg-11-3941-2014>.
- Valavi, R., Elith, J., Lahoz-Monfort, J.J., Guillera-Aroita, G., 2019. *blockCV: an R package for generating spatially or environmentally separated folds for k-fold cross-validation of species distribution models*. *Methods Ecol. Evol.* 10, 225–232. <https://doi.org/10.1111/2041-210X.13107>.
- Vellend, M., 2010. Conceptual synthesis in community ecology. *Q. Rev. Biol.* 85, 183–206. <https://doi.org/10.1086/652373>.
- Victorero, L., Robert, K., Robinson, L.F., Taylor, M.L., Huvenne, V.A.I., 2018. Species replacement dominates megabenthos beta diversity in a remote seamount setting. *Sci. Rep.* 8, 4152. <https://doi.org/10.1038/s41598-018-22296-8>.
- Walbridge, S., Slocum, N., Pobuda, M., Wright, D., 2018. Unified geomorphological analysis workflows with Benthic Terrain Modeler. *Geosciences* 8, 94. <https://doi.org/10.3390/geosciences8030094>.
- Warren, D.L., Glor, R.E., Turelli, M., 2008. Environmental niche equivalency versus conservatism: quantitative approaches to niche evolution. *Evolution* 62, 2868–2883. <https://doi.org/10.1111/j.1558-5646.2008.00482.x>.
- Warren, D.L., Matzke, N.J., Iglesias, T.L., 2020. Evaluating presence-only species distribution models with discrimination accuracy is uninformative for many applications. *J. Biogeogr.* 47, 167–180. <https://doi.org/10.1111/jbi.13705>.
- Wei, C.-L., González-Irusta, J., Domínguez-Carrió, C., Morato, T., 2020. Set of Terrain (Static in Time) and Environmental (Dynamic in Time) Variables Used as Candidate Predictors of Present-Day (1951–2000) and Future (2081–2100) Suitable Habitat of Cold-Water Corals and Deep-Sea Fishes in the North Atlantic. *PANGAEA*. <https://doi.org/10.1594/PANGAEA.911117>.
- Wood, S.N., 2011. Fast stable restricted maximum likelihood and marginal likelihood estimation of semiparametric generalized linear models. *J. R. Stat. Soc. Ser. B Stat. Methodol.* 73, 3–36. <https://doi.org/10.1111/j.1467-9868.2010.00749.x>.
- Woolley, S.N.C., Tittensor, D.P., Dunstan, P.K., Guillera-Aroita, G., Lahoz-Monfort, J.J., Wintle, B.A., Worm, B., O'Hara, T.D., 2016. Deep-sea diversity patterns are shaped by energy availability. *Nature* 533, 393–396. <https://doi.org/10.1038/nature17937>.
- Yesson, C., Taylor, M.L., Tittensor, D.P., Davies, A.J., Guinotte, J., Baco, A.R., Black, J., Hall-Spencer, J.M., Rogers, A.D., 2012. Global habitat suitability of cold-water octocorals. *J. Biogeogr.* 39, 1278–1292. <https://doi.org/10.1111/j.1365-2699.2011.02681.x>.
- Zibrowius, H., Cairns, S.D., 1992. Revision of the Northeast Atlantic and Mediterranean Stylasteridae (Cnidaria: Hydrozoa).